Title

Transcriptomics of SGLT2-positive early proximal tubule segments in mice: response to type 1 diabetes, SGLT1/2 inhibition, or GLP1 receptor agonism

Journal

American Journal of Physiology-Renal Physiology, 328(1)

ISSN

1931-857X

Authors

Kim, Young Chul

Das, Vivek

Kanoo, Sadhana

et al.

Publication Date

2025

DOI

10.1152/ajprenal.00231.2024

Transcriptomics of SGLT2-positive early proximal tubule segments in mice: response to type 1 diabetes, SGLT1/2 inhibition or GLP1 receptor agonism

Young Chul Kim[1,2]*, Vivek Das[3], Sadhana Kanoo[1,2], Huazhen Yao[4], Stephanie M. Stanford[5], Nunzio Bottini[5], Anil Karihaloo[7], Volker Vallon[1,2,6]*

* Contributed equally

[1]Division of Nephrology & Hypertension, Department of Medicine, University of California San Diego, La Jolla, CA, USA

[2]VA San Diego Healthcare System, San Diego, CA, USA

[3]Novo Nordisk A/S, Søborg, Denmark

[4]Institute for Genomic Medicine, University of California San Diego, La Jolla, CA, USA

[5]Division of Rheumatology, Allergy & Immunology, Department of Medicine, University of California San Diego, La Jolla, CA, USA

[6]Department of Pharmacology, University of California San Diego, La Jolla, CA, USA

[7]Novo Nordisk 33 Hayden Ave, Lexington, MA 02421 USAUSA

Corresponding author:

Volker Vallon; Division of Nephrology & Hypertension, Department of Medicine,

University of California San Diego & VA San Diego Healthcare System

3350 La Jolla Village Drive (9151), San Diego, CA 92161

Phone: 001-858-552-8585 ext. 5945; E-mail: vvallon@health.ucsd.edu

Abstract

SGLT2 inhibitors (SGLT2i) and GLP1 receptor (GLP1R) agonists have kidney protective effects. To better understand their molecular effects, RNA sequencing was performed in SGLT2-positive proximal tubule segments isolated by immunostaining-guided laser capture microdissection. Male adult DBA wildtype (WT) and littermate diabetic Akita mice ± Sglt1 knockout (Sglt1-KO) were given vehicle or SGLT2i dapagliflozin (dapa; 10mg/kg diet) for 2 weeks, and other Akita mice received GLP1R agonist semaglutide (sema; 3nmol/[kg body weight*day], s.c.). Dapa (254±11mg/dL) and Sglt1-KO (367±11mg/dL) but not sema (407±44mg/dL) significantly reduced hyperglycemia in Akita mice (480±33mg/dL). The 20,748 detected annotated protein-coding genes included robust enrichment of S1-segment marker genes. Akita showed 198 (~1%) differentially expressed genes vs. WT (DEGs; adjusted $p \leq 0.1$) including downregulation of anionic transport, unsaturated fatty acid and carboxylic acid metabolism. Dapa changed only 2 genes in WT but restored 43% of DEGs in Akita, including upregulation of lipid metabolic pathway, carboxylic acid metabolism and organic anion transport. In Akita, sema restored ~10% of DEGs, and Sglt1-KO and dapa were synergistic (restored ~61%) possibly involving additive blood glucose effects (193±15mg/dl). Targeted analysis of transporters and channels (t-test $p<0.05$) revealed that ~10% of 526 detectable transporters and channels were downregulated by Akita, with ~60% restored by dapa. Dapa, dapa+Sglt1-KO and sema also altered Akita-insensitive genes. Among DEGs in Akita, ~30% were unresponsive to any treatment, indicating potential new targets. In conclusion, SGLT2i restored transcription for multiple metabolic pathways and transporters in SGLT2-positive proximal tubule segments in diabetic mice, with a smaller effect also observed for GLP1R agonism.

New & Noteworthy (75 words)

SGLT2 inhibitors and GLP1 receptor agonists have kidney protective effects. By combining immunostaining guided laser-capture microdissection and RNA sequencing, the study established how the gene expression profile changes in SGLT2-positive proximal tubule cells in response to type 1 Akita diabetes and to pharmacological intervention by SGLT2 inhibition or GLP1R agonism and genetic deletion of SGLT1. The data also indicate genes unresponsive to those treatments that may include new therapeutical candidates.

Key words

SGLT2 inhibitor, Glucagon-like peptide-1 receptor agonist, Proximal tubule, RNA-seq, Laser capture microdissection

Introduction

Chronic kidney disease (CKD) is one of the leading causes of death and affects more than 800 million peoples worldwide (1). Diabetes is a common cause of CKD, and patients with diabetes and CKD are at high risk of kidney failure and cardiovascular events. To achieve better glycemic control in diabetes, new classes of drugs have been introduced in recent years (2). Sodium glucose cotransporter 2 inhibitors (SGLT2i) have demonstrated glucose-lowering effects and kidney and heart protection in clinical trials, thus becoming first-line drug therapy for people with type 2 diabetes and CKD (3, 4). Glucagon-like peptide-1 receptor (GLP1R) agonists are also glucose-lowering drugs with proven cardiovascular benefits as well as renoprotection (5) and have been recommended as second-line therapy (4). Despite growing evidence of beneficial effects on renal and cardiovascular outcomes, the underlying molecular mechanisms of SGLT2i and GLP1R agonists have not been fully understood.

The kidneys contribute to glucose homeostasis by filtering, reabsorbing, producing and consuming glucose. More than 95% of filtered glucose is reabsorbed by SGLT2 in the early proximal tubule and the rest is taken up by SGLT1 expressed in the late proximal tubule and thick ascending limb, such that only 0-0.2% of filtered glucose is excreted in the urine in healthy conditions. In diabetes, hyperglycemia increases the tubular glucose reabsorption by increasing the filtered glucose load and the transport capacity (the latter by increasing SGLT2 expression/activity in part due to growth and hypertrophy of the proximal tubule), thereby enhancing the tubular transport workload and facilitating tubular damage (6-9). The hyper-reabsorption of glucose, sodium and other electrolytes in the proximal tubule lessens the luminal NaCl delivery to the macula densa and the physiology of tubuloglomerular feedback (TGF) contributes to glomerular hyperfiltration, which has been linked to kidney function decline in the long term (10). Vice versa, SGLT2i acutely lowers GFR by attenuating proximal tubule hyper-reabsorption, which helps to preserve GFR in the long term (7, 11). Moreover, SGLT2i may protect tubular function by suppressing glucotoxicity, oxidative stress, and metabolic perturbation in diabetes partly by inhibiting mTORC1 signaling as well as improving autophagy in the proximal tubule (7, 12-16). However, little is known about the effect of diabetes and SGLT2i on the gene expression profile of the SGLT2i-targeted SGLT2-positive proximal tubule segments.

GLP1 is an incretin hormone secreted from intestinal L cells after mealtime and regulates glucose metabolism by inducing insulin secretion from pancreatic β-cells where its receptor GLP1R is highly expressed (17). GLP1R is a G-protein coupled receptor linked to cAMP-PKA

signaling. GLP1R mRNA expression has been detected in multiple tissues in rodents and human including lung, stomach, kidney and brain, contributing to GLP1's pleiotropic physiological effects such as gastric emptying and appetite control (18-22). Later studies using validated antibodies showed that GLP1R expression is rather limited to specific cell types in the tissues, and in human and rat kidneys it appears predominantly expressed in smooth muscle cells of the afferent arterioles (23, 24). Nonetheless, acute infusion of GLP1R agonists led to increase of GFR and renal blood flow, as well as natriuresis and diuresis associated with suppression of proximal tubule reabsorption in healthy and diabetic rodents (25-28). Furthermore, GLP1R knockout Akita mice showed increased urinary albumin and more advanced mesangial expansion compared with wildtype Akita mice, whereas GLP1R agonist treatment mitigated those conditions in Akita mice, consistent with protective kidney effects of GLP1R signaling (21). Vasodilatory effects of GLP1R-cAMP-PKA signaling on glomerular arterioles may contribute these outcomes (29), but the molecular mechanism by which GLP1R agonists modulates proximal tubule reabsorption and affects gene expression profile in the proximal tubule are not fully understood.

In the present study, we established transcriptomic profiles of SGLT2-positive proximal tubules, isolated by immunostaining-guided laser capture microdissection using a Sglt2 KO validated antibody. This was done in non-diabetic and type 1 diabetic Akita mice treated with SGLT2i or GLP1R agonist. In contrast to SGLT2 expression, SGLT1 is primarily expressed in the late proximal tubule, which is SGLT2-negative, and little effects should be observed in the microdissected segments by inhibiting SGLT1. Thus, mice with a gene knockout of SGLT1 were included in the study for comparison and as a kind of negative control, although SGLT1 inhibition could induce indirect effects, e.g. by lowering blood glucose in Akita mice. Pathway analysis was performed to determine: 1) effects of diabetes, 2) effects of SGLT2i in non-diabetic and diabetic conditions, 3) effects of Sglt1 deletion in non-diabetic and diabetic conditions, 4) whether combined SGLT2i and Sglt1 deletion has additive effects, and 5) whether a GLP1R agonist alters gene expression in the SGLT2-positive tubule in diabetes.

Materials and Methods

Animals

All animal experiments were conducted in accordance with the Guide for Care and Use of Laboratory Animals (National Institutes of Health, USA) and was approved by the local Institutional Animal Care and Use Committee as well as Novo Nordisk Animal Care and Use Committee. The generation of *Sglt1*$^{+/-}$*;Ins2*$^{Akita/+}$ on DBA/2J genetic background has been described (30, 31). Littermate experimental male mice were generated from breeding DBA/2J-*Sglt1*$^{+/-}$ to *DBA/2J- Sglt1*$^{+/-}$*;Ins2*$^{Akita/+}$. The mice were housed in the VA San Diego Health System vivarium with a 12:12 hour light-dark cycle and had free access to water and diet. The diet fed to all animals in the study had a minimal content of glucose and galactose to prevent diarrhea in Sglt1 KO mice, and high content of fructose (40% fructose by weight; TD.150497, Envigo, USA) to establish robust hyperglycemia in the absence of dietary glucose (30).

At ~14 weeks of age, the mice were treated for 2 weeks with dapagliflozin (10mg/kg diet) or semaglutide (one week acclimation with escalating doses of 1, 2 and finally 3nmol/kg bw daily via subcutaneous injection). Blood glucose was measured one day before treatment and 2 weeks later before harvest in awake mice by tail snip, and urine samples were collected at the same time points by inducing spontaneous urination with gentle grapping. Subsequently and under terminal anesthesia (ketamine (100 mg/kg) and xylazine (10 mg/kg) cocktail), the kidneys were perfused with cold saline through the left ventricle of the heart, quickly removed, and half kidney was immediately embedded in OCT compound in liquid nitrogen-chilled isopentane and stored in -80°C. All specimens were collected between 9 to 11 am to minimize variability due to circadian rhythm.

Urine and blood analysis

Glucose levels in urine samples were determined by the hexokinase/glucose-6-phosphate dehydrogenase method (Infinity Glucose Hexokinase Liquid Stable Reagent, ThermoFisher Scientific, USA), and urine creatinine concentration was determined by a kinetic modification of the Jaffe's reaction (Infinity Creatinine Reagent, ThermoFisher Scientific, USA). Blood glucose levels were determined by AlphaTRAK-2 glucometer (Abbott laboratories, USA).

Laser capture microdissection of SGLT2-positive early proximal tubules

10μm frozen kidney tissue sections were prepared and mounted on PEN membrane glass slides (cat# LCM0522, ThermoFisher Scientific, USA) and the tissue was fixed in ice-cold

acetone for 2 min. After brief air drying and rinsing the slide with RNase-free PBS (ThermoFisher Scientific, USA), the tissue was incubated with a KO-validated rabbit polyclonal SGLT2 antibody (32)(cat# 20802, BiCell Scientific, USA) for 10 min (1:100 in antibody solution: 5% normal goat serum + RNasin (400 unit/ml, Promega, USA) in PBS) at room temperature. After brief rinsing with PBS 2 times, the tissue was incubated with Alexa Fluor 555-conjugated anti-rabbit IgG antibody (1:100 in antibody solution, cat# A21428, ThermoFisher Scientific, USA) for 10 min at room temperature. After washing with PBS, the tissue was dehydrated by incubating in 70, 95 and 100% ethanol for 30 seconds each and in xylene for 5 min, and then completely dried in a fume hood. The SGLT2-positive tubules were located by fluorescent microscopy and then isolated using an Arcturus-XT laser capture microdissection system (ThermoFisher Scientific, USA).

RNA preparation and sequencing

Total RNA was isolated from ~70-80 microdissected SGLT2-positive tubules per sample via Arcturus PicoPure frozen RNA isolation kit (cat# KIT0204, ThermoFisher Scientific, USA) and additional gDNA digestion was performed using Arcticzymes Heat & Run gDNA removal kit (ArcticZymes Technologies, USA). Quality and quantity of the isolated RNAs were determined by High Sensitive RNA Screen Tape Analysis (Agilent, USA), and cDNA library was prepared using SMARTer Stranded Total RNA-seq Kit v3-Pico Input Mammalian (Takara Bio USA, USA) with 0.5 ng total RNA (DV200>30%). Sequencing of 50 million reads per sample was performed using Illumina NovaSeq 6000 (Illumina, USA) at the UC San Diego IGM Genomics Center.

Western blot

Whole kidney tissue was homogenized, and membrane fraction was prepared as previously described (12). SDS-PAGE was performed using 50 μg of proteins, and the proteins were transferred to PVDF membrane. The membrane was incubated overnight with primary antibodies at 4°C followed by incubation of HRP-conjugated secondary antibodies for 1hr at room temperature. The membrane was incubated with enhanced chemiluminescent substrate. The chemiluminescent signal was scanned by Chemdoc imaging system (Bio-Rad Laboratories), and the images were analyzed using Image Lab Software (Bio-Rad Laboratories). Primary antibodies used in this study were: anti-SLC22A2 antibody (PA5-80015, Invitrogen, 1:1,000), anti-SLCO1A1 antibody (BS-0607R, Bioss, 1:1,000), anti-SLC17A1 antibody (20751-1-AP, Proteintech, 1:1,000), anti-Vinculin antibody (66305-1-Ig, Proteintech, 1:10,000).

Bioinformatics analysis

For quality control MultiQC version 1.8. was used. All RNASeq samples were aligned using GRCm38 reference genome using bulk RNASeq workflow in Seven Bridges using SBG Create Expression Matrix CWL1.0 workflow. Alignment and quantification were done using Salmon. Gene symbol mapping was performed using EnsDb.Mmusculus.v79. The normalized data were checked for variance contribution and outlier detection using principal component analysis (PCA). 6/54 samples were detected as outliers after PCA using *prcomp* function with all available phenotypic covariates in the study design. Visualization for all explanatory phenotypic variables for variance explanation was performed using *ggplot2* function. Overall, 48 samples were selected for any subsequent downstream comparative analysis using DESeq2 to summarize transcript-level estimates for gene-level analysis with covariate of interest in R version 4.2 and BioC version 3.15. For all differential expression comparison statistical thresholds were set as p-adjusted ≤ 0.1 and $\log_2$ Fold change >0 or <0. PCA plots were done using *plotPCA* function available in DESeq2. Finally all pathway enrichment analysis was performed using ShinyGO 0.80 (33). The comparative assessment of overlapping differentially expressed genes across different pairwise comparative groups was done using Upset plot package.

Statistical analysis and plotting

Two-group comparisons of physiological parameters were performed by two-tailed t-test, and P <0.05 was considered as statistically significant. To perform a more permissive pathway analysis of differentially expressed genes between two groups, we used DESeq2 that uses Wald Test with multiple test adjusted p value (here ≤ 0.1 were used). For the targeted analysis of individual transporters and channels used to generate Supplemental Figures 1, 3 and 4, Wald Test with an adjusted p value ≤ 0.1 or a, less stringent, two-tailed t-test unadjusted p value < 0.05 was performed, the latter to capture a potential broader transporter response. Plots and heatmaps were generated by GraphPad Prism 10 or by Heatmapper (www.heatmapper.ca)(34).

Results

Study design and effect of treatment on physiological parameters

Fourteen-week old male mice (DBA-*Slc5a1*$^{+/+}$ *or* $^{-/-}$*; Ins2*$^{+/+}$ *or* $^{Akita/+}$) were divided into 9 groups (n=6 per group; **Table 1**) and were given vehicle (veh; control high fructose diet), dapagliflozin (Dapa; 10mg/kg diet), or semaglutide (escalating dose, see Methods) for 2 weeks. Body weight and mean kidney to body weight ratio (KW/BW) were not significantly changed by any of the treatments, except for a modestly higher KW/BW ratio in dapa-treated vs veh-treated Sglt1 KO mice (**Table 2**). In non-diabetic mice, Sglt1 KO and dapa modestly increased urinary glucose to creatinine ratios (UGCR) with a greater effect of the latter; moreover, UGCR was strongly increased by dapa in non-diabetic Sglt1 KO mice consistent with compensatory glucose reabsorption via SGLT1 when upstream SGLT2 is inhibited (30, 35). Despite these effects on glucose excretion, blood glucose was not significantly changed by Sglt1 KO or dapa in non-diabetic mice. In Akita mice, however, Sglt1 KO lowered baseline blood glucose (367±11mg/dL), and dapa, as expected, induced an even stronger reduction (254±11mg/dL) vs. vehicle-treated mice (480±33mg/dL); moreover, dapa further reduced blood glucose in Sglt1 KO Akita (193±15 mg/dL)(**Table 2**). Having the lowest blood glucose levels among Akita groups, dapa-treated Sglt1 KO Akita mice had the highest UGCR consistent with additive effects of SGLT2 and SGLT1 inhibition on glucose reabsorption in Akita mice (30)(**Table 2**). In comparison, blood glucose was numerically decreased by sema in Akita mice (407±44mg/dL) but this did not reach statistically significance.

RNA sequencing of SGLT2-positive proximal tubule segments collected by laser capture microdissection

After 2 weeks of treatment with dapa or sema, kidneys were harvested, frozen kidney sections prepared and immuno-stained with a Sglt2 knockout-validated (32) anti-SGLT2 antibody (**Fig. 1A**), and the SGLT2-positive segments were isolated by laser capture microdissection (LCM) from each experimental animal (**Fig. 1B**). RNA sequencing (RNA-seq) of these tissue samples allowed detection of a total of 20,748 annotated protein-coding genes. Enrichment of early proximal tubular segments was confirmed by comparing the RNA-seq data generated in vehicle-treated WT mice with previously generated RNA-seq data of microdissected mouse kidney tubule segments by the Knepper group (36): transcripts per million (TPM) in our LCM samples for proximal tubule S1 segment marker genes (including *Slc5a12, Slc4a4, Slc5a2, Slc22a8 and Prodh2* (37, 38)) were ~5-40% of TPM reported by the Knepper group, whereas TPM values for

marker genes of the S3 segment, ascending limb, distal convoluting tubule, connecting tubule and collecting duct were negligible (0~3% of the reference) (**Fig. 1C**).

Diabetes downregulates the expression of genes associated with fatty acid metabolism and transport in SGLT2-positive proximal tubule segments

The effect of diabetes was determined by comparing transcriptomics of non-diabetic WT mice and Akita mice. Principal component analysis (PCA) showed separation between the two groups (**Fig. 2A**). 198 genes were differentially expressed (DEGs; adjusted p<0.1 and log2 Fold change >0 or <0) between WT and Akita mice (63 up, 135 down; **Fig. 2B**, **Supplemental Table 1**). Pathway analysis with these DEGs revealed the enrichment of various metabolic processes, and the top 10 pathways (based on FDR <0.05 and fold enrichment score) were long-chain fatty acid metabolic process, unsaturated fatty acid metabolic process, organic anion transport, fatty acid metabolic process, anion transport, monocarboxylic acid metabolic process, carboxylic acid metabolic process, organic acid metabolic process, and oxoacid metabolic process (**Fig. 2C**). The DEGs in the metabolic processes were mostly downregulated in Akita vs WT mice with only a few being upregulated (**Supplemental Table 2**). Especially genes involved in fatty acid metabolic process were downregulated in SGLT2-positive proximal tubule segments of Akita mice (**Fig. 2D and Supplemental Table 2**). The 63 upregulated genes in Akita vs WT included genes associated with cell adhesion and extracellular matrix (*Adam11, Itgb6, Fn1* and *Npnt*), lipid metabolism and transport (*ApoB, Npl, Ephx1* and *Fabp3*) and cell cycle and proliferation (*Ctgf, Ccnd1, Ccng1* and *Lzts2*).

The SGLT2-positive early proximal tubule plays a critical role in the transport and reabsorption of ions, organic, and inorganic molecules. We found that several solute carrier (*Slc*) genes are among the DEGs between Akita vs WT (**Supplemental Table 2**). Therefore, we performed a targeted analysis for renal transporters and channels. For the targeted analysis, P value <0.05 (two-tailed t-test) was considered statistically significant. Among known 805 kidney transporters and channels (39)(https://esbl.nhlbi.nih.gov/helixweb/ Database/NephronRNAseq /Transporters_and_Channels.html), 525 genes had TPM>0 in the SGLT2-positive segment RNA-seq data (**Supplemental Table 3**) and 51 of them (~9.7%) were significantly changed in Akita vs WT mice (**Fig. 2E and Supplemental Table 4**). Notably, all those transporters, except 3 (*Slc3a2, Rhbg and Abca8a*), were downregulated in the diabetic mice, and 15 transporters (*Slco1a1, Slc7a13, Slc12a1, Slc35b4, Slc17a1, Slc3a2, Slc30a5, Kcnj15, Slc1a4, Slco3a1, Slc9a3, Slc6a9, Slc19a3, Slc12a2 and Slc22a21*) also met the untargeted DEGs analysis criteria (adjusted p<0.1). Unexpectedly, *Slc12a1* which encodes Na-K-2Cl Cotransporter 2

(NKCC2), the major apical sodium transporter in the thick ascending limb was in the list. Notably, *Slc12a1* mRNAs were detectable in the proximal tubule in RNA-seq analysis using microdissected tubule and single-nuclear RNA-seq analysis even though the expression level was significantly lower than the level in the thick ascending limb (36, 37).

Dapagliflozin largely restores gene expression in SGLT2-positive proximal tubule segments of the diabetic kidney

To determine the effect of dapa on the transcriptome of SGLT2-positive proximal tubule segments, we compared RNA-seq data in non-diabetic (WT+dapa vs WT) as well as diabetic mice (Akita+dapa vs Akita). In non-diabetic mice, dapa had a very limited impact on gene expression in these segments, and only 2 DEGs could be annotated (*Ugt2b37* and *Gm25679*, **Supplemental Table 5**), indicating that 2 week-inhibition of glucose reabsorption in SGLT2-positive proximal tubule segments did not induce robust gene expression changes in the absence of hyperglycemia.

In contrast, dapa induced robust effects on gene expression in the diabetic kidney. PCA showed clear separation between Akita and Akita+dapa (**Fig. 3A**), with 252 DEGs (159 up, 93 down; **Fig. 3B and Supplemental Table 6**). Pathway analysis showed that many pathways altered by Akita vs non-diabetic WT mice were also sensitive to dapa (**Fig. 3C**). In fact, 86 of the 198 genes affected by Akita (~43%) were significantly restored by dapa (**Fig. 3D and Supplemental Table 6**). This included genes in fatty acid metabolic processes which were mostly restored in Akita by dapa (**Supplemental Table 7**).

We recently reported the effects of dapa on kidney cortex protein expression in Akita mice by proteomics (12). To determine whether the gene expression changes in the SGLT2-positive segments by dapa in Akita can be translated to protein expression changes, we performed correlation analysis between the proteomics data and the RNA-seq data (**Fig. 3E**). Despite the differences in these two studies [genetic background (DBA vs C57Bl6), age (12 vs 10 weeks old), duration of treatment (2 vs 1 week) and diet (high fructose vs Western diet)], 159 genes of the 252 DEGs were detected in the proteomics analysis and 123 of the 159 genes (~77.4%) showed positive correlation with the protein expression changes. 22 of those (red dots, **Fig. 3E**) were also significantly changed in the proteomic analysis (adjusted $p<0.1$).

Gene expression of 30 of the 51 transporter genes (59%) altered in the SGLT2-positive proximal tubule segments of diabetic mice (**Fig. 2E**) were restored by dapa (**Fig. 3F and Supplemental Table 8**). This included transporters involved in apical and basolateral

membrane transport as well as in tight junctions, mitochondria, peroxisomes, endoplasmatic reticulum, endosome, and Golgi apparatus (**Supplemental Fig. S1)**.

Dapa significantly increased the expression of additional 33 transporter genes that were not significantly changed by Akita vs WT (**Fig. 3H)** with a similar broad transporter localization (**Supplemental Fig. S1**). Taken together, 2 weeks of dapa treatment restored to a significant extent the gene expression of lipid metabolic pathway genes and transporters in SGLT2-positive proximal tubule segments of diabetic mice, whereas its effect on gene expression in non-diabetic mice was marginal.

To determine whether observed reductions in mRNA levels of transporters in the early proximal tubules in Akita mice and their restoration by dapa may translate to membrane protein expression, we performed Western blot analysis on available whole kidneys for 3 transporters that in the kidney are all primarily expressed along the proximal tubules (https://esbl.nhlbi.nih.gov/MRECA/Nephron/): the primarily basolaterally localized organic cation transporter OCT2 (SLC22A2) and organic-anion-transporting polypeptide Oatp1a1 (SLCO1A1) as well as the apically localized urate and anion exporter NPT1 (SLC17A1). Western blotting on the whole kidney membrane level confirmed decreased protein expression of the 3 transporters in Akita vs. nondiabetic mice. Dapa showed a non-significant trend to restore whole kidney membrane protein expression of SLCO1A1 but did not alter the expression of SLC22A2 or SLC17A1 (**Supplemental Fig. S2**). See Discussion for interpretation.

Effect of semaglutide on SGLT2-positive proximal tubule transcriptome in diabetes

Despite lack of robust evidence for GLP1R expression in renal tubular cells, GLP1R agonists have shown to affect proximal tubular function and induce renoprotection in diabetic kidney disease (21, 22, 26-28). Thus, we determined the effects of semaglutide (sema), a GLP1R agonist, on the transcriptome of SGLT2-positive segments in Akita mice. The comparison of Akita+sema and Akita RNA-seq data produced 64 DEGs (41 up, 23 down; **Fig. 4A, Supplemental Table 9**). Pathway analysis showed partial restorations of genes in organic acid, oxoacid and carboxylic acid metabolic process, organic anion transport and lipid metabolism, and enrichment of genes associated with response to glucose/hexose (**Fig. 4B and Supplemental Table 10**). 20 genes affected by Akita were restored by sema (up by sema: *Hdc, Nampt, Dnajc3, Sec63, Mgam, Eif4b, Sugct, Zbtb20, Wwp1, Ctbs, Zfp110*; down: *Zfp697, Palm3, Nckap5, Stmtn, Mthfr, Llgl2, Tubb4b, Npnt, Aen*)(**Supplemental Table 9, Supplemental Fig. S3**). We also performed targeted analysis for transporters (P value <0.05, two-tailed t-test),

which identified 28 transporters being significantly changed by sema in Akita mice (26 up and 2 down) including the restoration of gene expression for 15 transporters compared with Akita (red box in **Fig. 4D, Supplemental Table 11 and Supplemental Fig. S4**). Notably, 11 out of the 15 restored transporters were regulated in the same way by sema and dapa (asterisks, **Fig. 4D**). Moreover, among 13 additional transporter genes changed by sema but not by Akita, 5 were regulated in the same way by sema and dapa. Thus, despite a proposed indirect effect on the proximal tubule and an at most modest effect of sema on blood glucose in Akita mice, sema treatment induced a remarkably similar effect to dapa on early proximal tubule transporter gene expression.

Limited effect of SGLT1 knockout on SGLT2-positive proximal tubule transcriptome

In the kidney, SGLT1 is expressed at the apical membrane of the S2/S3 segment of proximal tubule, the thick ascending limb and the macular densa, and reabsorbs ~3% of the filtered glucose in healthy condition (11). The effect of SGLT1 inhibition on the SGLT2-positive proximal tubule segment transcriptome in non-diabetic and diabetic mice was determined by comparing Sglt1 knockout (KO) vs WT as well as Sglt1 KO Akita vs Akita. In non-diabetic mice, Sglt1 KO significantly changed 22 genes (3 up; 19 down, incl. *Slc5a1* or *Sglt1* as expected) compared with WT (**Supplemental Table 12**), while 13 genes were differentially expressed between Sglt1 KO Akita vs Akita (6 up, 7 down, incl. *Slc5a1* or *Sglt1*)(**Fig. 4E and Supplemental Table 13**). Among the DEGs, 3 genes (*Cd36, Llgl2 and Hdc*) were restored by Sglt1 KO in Akita (**Supplemental Table 13**). Neither set of DEGs led to significant pathway enrichment, but *Abhd1* was upregulated by Sglt1 KO in both non-diabetic and diabetic mice. Little is known about this α/β hydrolase membrane protein, which may inhibit oxidative stress (40). Targeted analysis for transporters in diabetes (P value <0.05; two-tailed t-test) showed that 7 transporters were significantly changed (5 up; 2 down) and downregulation of *Cacna1d* in Akita was restored by Sglt1 KO (**Fig. 4F and Supplemental Table 14**). This gene codes for an L-type, voltage-activated calcium channel with polymorphisms being associated with increased blood pressure and salt sensitivity of blood pressure (41). A lesser effect of Sglt1 KO vs dapa in Akita was not unexpected based on a lesser effect on blood glucose and little expression of SGLT1 in the early proximal tubules.

Additive effects of Sglt1 KO and SGLT2 inhibition on SGLT2-positive proximal tubule transcriptome in diabetes

Exploring the combined effects of Sglt1 KO and SGLT2 inhibition on the SGLT2-positive proximal tubule transcriptome, in non-diabetic mice only 3 genes were differentially expressed compared with WT (1 up; 2 down, including *Slc5a1* or *Sglt1*), arguing against an additive effect of combined inhibition in the non-diabetic setting (**Supplemental Table 15**). In diabetes, however, Sglt1 KO and SGLT2 inhibition were synergistic. PCA showed distinct separation between Sglt1 KO Akita+dapa vs Akita (**Fig. 5A**) with 453 DEGs (273 up, 180 down; **Fig. 5B and Supplemental Table 16**). About 61% of genes deregulated by diabetes (121 out of 198) were restored by combined inhibition (**Fig. 5C and Supplemental Table 16**); for comparison, dapa and Sglt1 KO had restored ~43% and 1.5%, respectively (see above). Pathway enrichment analysis revealed more restored pathways (incl. protein exit from endoplasmic reticulum and amino acid transport) and additional enriched pathways (incl. sodium ion transport and negative regulation of intrinsic apoptotic signaling pathway) versus dapa alone (**Fig. 5D and Supplemental Table 17**). Moreover, transcripts of 63 transporter genes were changed by Sglt1 KO+dapa in Akita and ~55% of affected transporters in Akita trended towards normal (**Fig. 5E and Supplemental Table 18**), which is close to the ~58% restored by dapa only (see above). Taken together, in diabetic mice dual inhibition of SGLT1 and SGLT2 has a greater effect on blood glucose as well as the SGLT2-positive proximal tubule transcriptome than SGLT2 inhibition alone, primarily on non-transporter related genes, whereas the combined inhibition has very little effect in non-diabetic mice.

Potential new targets in the diabetic early proximal tubule

To identify new potential therapeutic targets in the SGLT2-positive early proximal tubule we probed for genes that are dysregulated by diabetes but not significantly changed in diabetic mice by dapa, sema, Sglt1 KO, or Sglt1 KO+dapa and found 61 genes that satisfy the criteria (**Fig. 6A, Supplemental Table 19**). Pathway analysis with those 61 genes revealed one significantly enriched pathway: response to glucagon (FDR<0.05, **Fig. 6B**). Moreover, targeted analysis for transporters identified 14 transporters that were changed by diabetes (2 up (Slc3a2, Rhbg) and 12 down) and not significantly changed in diabetic mice by any of the treatments (**Fig. 6C**).

Discussion

The kidney is a complex machinery that regulates the urinary excretion of fluid and many solutes depending on the homeostatic needs of the organism, including electrolytes, acid and base equivalents, and small molecules like nitrogenous compounds and metabolites. To accomplish this goal, the kidney tubule system consists of at least 14 distinct and micro-dissectible segments (36), each with a specialized cell function and implications for kidney physiology and pathophysiology. The kidney has evolved in a way that a large fraction of the filtered fluid and solutes is reabsorbed in the early proximal tubule, associated with a high oxygen need and mitochondrial density (42). This segment is also the site of apical membrane expression of SGLT2, the primary pathway for kidney glucose reabsorption and target of SGLT2i, which demonstrated robust kidney protection in large clinical outcome trials in diabetic and non-diabetic individuals (9). To gain a deeper understanding of this segment, we have established transcriptional profiles of the SGLT2-postitive early proximal tubule to study the response to Akita diabetes, SGLT2i, Sglt1 KO and GLP1R agonist. To this end, we performed laser capture microdissection (LCM) on frozen kidney tissue samples. LCM is a tool to isolate a distinct cell population based on histological morphology or specific protein expression without introducing stress responses due to enzymatic or mechanical tissue dissociation and has been successfully used for determining renal segment-specific gene expression profiles in health and disease (43-45). By combining immunostaining-guided LCM utilizing a Sglt2 KO-validated SGLT2 antibody (32) with RNA-seq analysis, we were able to detect 20,748 protein-coding genes in this segment of interest.

We found that Akita diabetes changed the expression of ~1% of genes in the SGLT2-positive proximal tubule. The SGLT2i dapa altered 1.2% of genes in Akita and induced opposite effects to Akita in 43% of these genes. Combining SGLT2i with Sglt1 KO changed 2.2% of genes in Akita and restored 61% of the Akita-altered genes, showing synergistic effects of SGLT2+SGLT1 inhibition on both gene expression as well as blood glucose control (**Fig. 6D**). Defective fatty acid oxidation in renal tubule has been linked to CKD in human and rodents (46-49). Additionally, in animal models of diabetic kidney disease (DKD), lipid metabolism was suppressed in proximal tubules, and this was reversed by SGLT2i treatment (13, 14, 50). In line with this, we found that genes involved in lipid and fatty acid metabolism were downregulated in SGLT2-positive proximal tubules of Akita mice; moreover, two weeks of dapa treatment or combination of Sglt1 KO and dapa treatment reversed this effect (**Fig. 2C, 3C, 5D, Supplemental Table 2, 7 and 17**). These data indicate that the described metabolic shift in the

proximal tubule is a consequence of SGLT2-mediated glucose uptake and/or secondary to hyperglycemia, since, as expected, SGLT2i and combined SGLT2i+Sglt1 KO had a significant blood glucose lowering effect in the Akita mice. Comparison of the dapa effect in Akita based on RNA-seq data in the SGLT2-positive proximal tubule in the current study with the response to dapa in Akita assessed in a recent proteomics analysis of the kidney cortex (12) showed a positive correlation (**Fig. 3E**), validating to some extent the RNA-seq analysis at the protein level.

In comparison, dapa treatment had little effect on the gene expression (2 DEGs) in SGLT2-positive segments in non-diabetic WT mice (**Supplemental Table 5**). This observation is in contrast to the above-mentioned proteomics study, which showed a robust effect of dapa treatment on kidney cortex protein expression in WT mice (12). The differences could be related to the used diet (glucose-free & high fructose vs Western diet) that could affect the tubular responsiveness but might also be due to differences in how the early proximal tubule cells respond to blockade of glucose reabsorption via SGLT2 on the mRNA versus protein level as well as in normoglycemia versus hyperglycemia. Metabolic adaptation through primary effects at the protein level, such as degradation, recycling or post-translational modifications, are more energy efficient than by changing gene expression, and thus may be the first line of response in normoglycemia. Also, while many of the genes affected in the proteomics study by dapa in WT mice are primarily expressed in early proximal tubules (S1/S2 segments), others are primarily expressed in the later proximal tubule (S2/3) or other tubular segments, and would possibly not be captured in the present study. Moreover, the downstream shift in transport of glucose and other substrates in response to SGLT2i is a hallmark of these drugs and expected to induce opposite responses in SGLT2-positive versus the downstream SGLT2-negative segments (9, 12), the latter not being captured in the current study. On the other hand, in diabetes, where a better correlation is observed between RNA-seq and proteomics responses to dapa, the more efficient regulation on the protein level may no longer be prioritized. Moreover, since glucose transport in SGLT2-negative S2/S3 segments is saturated in glucosuric Akita mice, even before SGLT2i treatment, fewer opposing effects on gene/protein expression are expected in SGLT2-negative S2/3 versus SGLT2-positive S1/S2 segments, which may also contribute to the observed better correlation between mRNA responses in early proximal tubules and protein responses assessed in kidney cortex.

Our targeted analysis for transporters indicated reduced mRNA levels of ~10% of transporters and channels in the diabetic early proximal tubule (**Fig. 2E**), including multiple cellular domains

(**Supplemental Fig.S1**), which was likewise largely restored by dapa or Sglt1 KO+dapa (**Fig. 3F and 5E**). Three plasma membrane transporters (SLCO1A1, SLC22A2, SLC17A1) primarily expressed along the proximal tubule and showing the described mRNA response to Akita and dapa, were chosen for Western blotting on whole kidney membrane fractions. Like the early proximal mRNA response, Akita reduced whole kidney membrane protein expression for all 3 transporters (**Supplemental Fig.S2**). Decreased expression of plasma membrane transporters in the diabetic proximal tubule seems at first unexpected based on proximal tubule hypertrophy and hyperreabsorption in early diabetes (10). However, the latter may primarily relate to glucose transport, whereas the relatively small number of transporters showing reduced mRNA expression in the current study were not related to glucose transport. In accordance, a previous study showed an increase in total kidney membrane protein expression of SGLT2 in Akita mice vs non-diabetic controls whereas the expression of another prominent early proximal sodium transporter, the Na/H-exchanger NHE3, was unchanged (51). A recent single cell RNA-seq analysis of S1 proximal tubular cells of humans with uncomplicated type 2 diabetes mellitus (16) did not show the transporter mRNA downregulation observed in the current study. Considering the robust impact of insulin on early proximal tubule function, this could relate to the nature of the Akita model, which is characterized by hypoinsulinemia in contrast to individuals with hyperinsulinemic type 2 diabetes. Dapa showed a trend to restore whole kidney membrane protein expression of SLCO1A1 in Akita but did not affect SLC22A2 or SLC17A1. The dissociation between mRNA expression in S1/2 segments and whole kidney protein expression in response to dapa could relate to the induced shift of transport of sodium, glucose, and fluid, but also additional substrates (12), from the S1/2 to S3 segments, which may induce opposing effects on these segments. All 3 transporters are expressed in S1, S2 and S3 segments of the murine proximal tubule, but their fractional S3 mRNA expression differs, with ~30% for Slc22a2 and Slc17a1, but only 10% for Slco1a1, which may explain the lesser dissociation. Determination of proteomic profiles in SGLT2-positive early proximal tubules isolated the same way by LCM will be helpful to follow up this hypothesis, as will be similar studies in SGLT2-negative S2/S3 segments to show potential opposite effects of SGLT2i on gene and protein expression.

Sglt1 KO alone had little effect on gene expression of SGLT2-positive proximal tubules even in the diabetic kidney despite a significant blood glucose reduction (8 DEGs including *Slc5a1*; **Fig. 4E, Table 2 and Supplemental Table S13**), suggesting that inhibition in late proximal tubule glucose transport via SGLT1 and the modest lowering in blood glucose by Sglt1 KO in Akita (367 vs 480 mg/dL) do not have a strong regulatory impact on gene expression in the upstream

early proximal tubule. In contrast, sema, which had a smaller blood glucose effect (407 mg/dL) than Sglt1 KO, altered 64 genes in the SGLT2-positive proximal tubule in Akita mice (**Fig. 4A and Supplemental Table 9**), suggesting blood glucose-independent effects of sema. This included the reversal in expression of 20 Akita-altered genes linked to metabolism, transcription regulation, inflammation, and the cytoskeleton (**Supplemental Fig. S3**). The gene expression effect of sema in Akita included multiple transporters, and, remarkably, multiple transporters were changed in the same direction by dapa and sema (**Supplemental Fig. S4**). In the kidney, the GLP1R is mainly expressed in the smooth muscle cells of afferent arterioles, where its activation by GLP1R agonists can induce vasodilation and an increase in GFR and natriuresis in rodents and humans (22). How the GLP1R agonist can affect gene expression in early proximal tubules remains unclear. We previously found that the GLP1R agonist-induced natriuresis is associated with increased kidney phosphorylation and thus inhibition of the Na-H-exchanger NHE3, a primary pathway for sodium reabsorption in the early proximal tubule (27), but, again, the effects on the tubules could have been direct or indirect. A hypothesis would be that the GLP1R-cAMP-PKA signaling in the vascular smooth muscle cells of the afferent arteriole may release paracrine factors to regulate the function of the early proximal tubule cells. Or dapa and sema induce similar systemic effects beyond glucose control that can impinge on the kidney. Further studies are needed to test such hypotheses.

Finally, the analysis identified 61 genes (including 12 transporters) the expression of which was changed by Akita but not significantly restored by either treatment (**Fig. 6A, Supplemental Table 19**). Pathway analysis revealed significant enrichment of the “response to glucagon” pathway, with upregulation of *Stk11* and downregulation of *Screbf1* and *Cdo1* in Akita (**Fig. 6B**). STK11 is a serine/threonine kinase implicated in glucose-sensitive control of glucagon secretion in the pancreas (52). Potentially more relevant to the diabetic proximal tubule, STK11 is the key upstream activator of the AMP-activated protein kinase (AMPK), a central metabolic switch that suppresses growth and proliferation when energy and nutrient levels are scarce (53). AMPK can phosphorylate the transcription factor SREBF1 thereby preventing the transcription of its target genes, including sterol synthesis (54). CDO1 (cysteine dioxygenase 1) is key enzyme for cysteine catabolism that can activate AMPK signaling to promote fatty acid oxidation and mitochondrial biogenesis, at least in hepatocytes to attenuate hepatosteatosis (55). Further studies are needed to determine how the reported mRNA expression data of these and the other 58 genes relate to protein expression and activity to gain a more cohesive picture that may indicate a potential role in the diabetic kidney or as novel therapeutic targets.

Limitations of this study include the use of a genetic type I diabetes model that primarily reflects the kidney response to suppressed insulin levels and the resulting hyperglycemia. The Akita model does not mimic the hyperinsulinemia typically found in patients with type 2 diabetes, but may mimic the setting of hypoinsulinemic humans with type 1 diabetes before they are treated with insulin. Moreover, the analysis is restricted to male mice. While the clinical outcome studies show comparable kidney protection by SGLT2i and GLP1R agonists in female and male individuals, sex affects gene and protein expression along the nephron and further comparative studies are needed.

In summary, by combining immunostaining guided LCM and RNA-seq, the present study established how the gene expression profile changes in SGLT2-positive proximal tubule cells in response to type 1 Akita diabetes and to pharmacological intervention by SGLT2i or GLP1R agonist and genetic deletion of SGLT1. The data provide new insights on the level of this prominent tubular segment for the responses to the clinically relevant and kidney protective drugs, dapa and sema, but also indicate genes unresponsive to those treatments that may include new therapeutical candidates, potentially including the glucagon pathway.

Acknowledgements

This publication includes data generated at the UC San Diego IGM Genomics Center utilizing an Illumina NovaSeq 6000 that was purchased with funding from a National Institutes of Health SIG grant (#S10 OD026929) and data generated at the UC San Diego Laser Capture Dissection Core that was funded by National Institutes of Health grant P30AR073761. We thank Anna Belongia for technical support of laser capture microdissection.

Conflict of Interest Statement

Over the past 24 months, V.V. has served as a speaker or consultant and received honoraria from Astra-Zeneca and Boehringer-Ingelheim, and received grant support for investigator-initiated research from Boehringer-Ingelheim, Gilead, Lexicon, Novo-Nordisk, and Maze Therapeutics. V.D. and A.K. are employees of Novo-Nordisk, which makes semaglutide. V.D. is also a member of the Scientific Advisory Board of Pythia Biosciences. None of the other authors has any conflicts of interest, financial or otherwise, to disclose.

Grant support

The authors were supported by National Institutes of Health (NIH) Grants R01 DK112042 (to V.V.), University of Alabama at Birmingham/University of California-San Diego O'Brien Center of Acute Kidney Injury NIH Grant U54 DK137307 (to V.V.), and the Department of Veterans Affairs. The study was supported by an investigator-initiated research project through Novo-Nordisk (to V.V.).

Supplemental material

Supplemental Figures S1-S4: doi.org/10.6084/m9.figshare.27623982

Supplemental Tables S1-S19: doi.org/10.6084/m9.figshare.26072950.v1.

Data and code availability

All fastq files and processed data file are openly available at the NCBI GEO with accession number GSE279174 (ncbi.nlm.nih.gov/geo/query/acc.cgi?acc=GSE279174).

The R code used in the analysis can be accessible at https://github.com/vd4mmind/AKITA_LCM_RNASeq_Treatment.

References

1. **Kovesdy CP**. Epidemiology of chronic kidney disease: an update 2022. *Kidney Int Suppl (2011)* 12: 7-11, 2022.
2. **Taylor SI, Yazdi ZS, and Beitelshees AL**. Pharmacological treatment of hyperglycemia in type 2 diabetes. *J Clin Invest* 131: 2021.
3. **Vallon V, and Kim YC**. Protecting the Kidney: The Unexpected Logic of Inhibiting a Glucose Transporter. *Clin Pharmacol Ther* 112: 434-438, 2022.
4. **Rossing P, Caramori ML, Chan JCN, Heerspink HJL, Hurst C, Khunti K, Liew A, Michos ED, Navaneethan SD, Olowu WA, Sadusky T, Tandon N, Tuttle KR, Wanner C, Wilkens KG, Zoungas S, Craig JC, Tunnicliffe DJ, Tonelli MA, Cheung M, Earley A, and de Boer IH**. Executive summary of the KDIGO 2022 Clinical Practice Guideline for Diabetes Management in Chronic Kidney Disease: an update based on rapidly emerging new evidence. *Kidney Int* 102: 990-999, 2022.
5. **Perkovic V, Tuttle KR, Rossing P, Mahaffey KW, Mann JFE, Bakris G, Baeres FMM, Idorn T, Bosch-Traberg H, Lausvig NL, Pratley R, Committees FT, and Investigators**. Effects of Semaglutide on Chronic Kidney Disease in Patients with Type 2 Diabetes. *N Engl J Med* 2024.
6. **Wang XX, Levi J, Luo Y, Myakala K, Herman-Edelstein M, Qiu L, Wang D, Peng Y, Grenz A, Lucia S, Dobrinskikh E, D'Agati VD, Koepsell H, Kopp JB, Rosenberg AZ, and Levi M**. SGLT2 Protein Expression Is Increased in Human Diabetic Nephropathy: SGLT2 PROTEIN INHIBITION DECREASES RENAL LIPID ACCUMULATION, INFLAMMATION, AND THE DEVELOPMENT OF NEPHROPATHY IN DIABETIC MICE. *J Biol Chem* 292: 5335-5348, 2017.
7. **Vallon V, Gerasimova M, Rose MA, Masuda T, Satriano J, Mayoux E, Koepsell H, Thomson SC, and Rieg T**. SGLT2 inhibitor empagliflozin reduces renal growth and albuminuria in proportion to hyperglycemia and prevents glomerular hyperfiltration in diabetic Akita mice. *Am J Physiol Renal Physiol* 306: F194-204, 2014.
8. **Hu Z, Liao Y, Wang J, Wen X, and Shu L**. Potential impacts of diabetes mellitus and anti-diabetes agents on expressions of sodium-glucose transporters (SGLTs) in mice. *Endocrine* 74: 571-581, 2021.
9. **Vallon V**. How can inhibition of glucose and sodium transport in the early proximal tubule protect the cardiorenal system? *Nephrol Dial Transplant* 2024.
10. **Vallon V, and Thomson SC**. Renal function in diabetic disease models: the tubular system in the pathophysiology of the diabetic kidney. *Annu Rev Physiol* 74: 351-375, 2012.
11. **Oe Y, and Vallon V**. The Pathophysiological Basis of Diabetic Kidney Protection by Inhibition of SGLT2 and SGLT1. *Kidney Dial* 2: 349-368, 2022.
12. **Billing AM, Kim YC, Gullaksen S, Schrage B, Raabe J, Hutzfeldt A, Demir F, Kovalenko E, Lasse M, Dugourd A, Fallegger R, Klampe B, Jaegers J, Li Q, Kravtsova O, Crespo-Masip M, Palermo A, Fenton RA, Hoxha E, Blankenberg S, Kirchhof P, Huber TB, Laugesen E, Zeller T, Chrysopoulou M, Saez-Rodriguez J, Magnussen C, Eschenhagen T, Staruschenko A, Siuzdak G, Poulsen PL, Schwab C, Cuello F, Vallon V, and Rinschen MM**. Metabolic Communication by SGLT2 Inhibition. *Circulation* 149: 860-884, 2024.
13. **Kogot-Levin A, Hinden L, Riahi Y, Israeli T, Tirosh B, Cerasi E, Mizrachi EB, Tam J, Mosenzon O, and Leibowitz G**. Proximal Tubule mTORC1 Is a Central Player in the Pathophysiology of Diabetic Nephropathy and Its Correction by SGLT2 Inhibitors. *Cell Rep* 32: 107954, 2020.
14. **Tomita I, Kume S, Sugahara S, Osawa N, Yamahara K, Yasuda-Yamahara M, Takeda N, Chin-Kanasaki M, Kaneko T, Mayoux E, Mark M, Yanagita M, Ogita H, Araki SI, and Maegawa H**. SGLT2 Inhibition Mediates Protection from Diabetic Kidney Disease by Promoting Ketone Body-Induced mTORC1 Inhibition. *Cell Metab* 32: 404-419 e406, 2020.

15. **Tanaka S, Sugiura Y, Saito H, Sugahara M, Higashijima Y, Yamaguchi J, Inagi R, Suematsu M, Nangaku M, and Tanaka T**. Sodium-glucose cotransporter 2 inhibition normalizes glucose metabolism and suppresses oxidative stress in the kidneys of diabetic mice. *Kidney Int* 94: 912-925, 2018.
16. **Schaub JA, AlAkwaa FM, McCown PJ, Naik AS, Nair V, Eddy S, Menon R, Otto EA, Demeke D, Hartman J, Fermin D, O'Connor CL, Subramanian L, Bitzer M, Harned R, Ladd P, Pyle L, Pennathur S, Inoki K, Hodgin JB, Brosius FC, 3rd, Nelson RG, Kretzler M, and Bjornstad P**. SGLT2 inhibitors mitigate kidney tubular metabolic and mTORC1 perturbations in youth-onset type 2 diabetes. *J Clin Invest* 133: 2023.
17. **Muskiet MHA, Tonneijck L, Smits MM, van Baar MJB, Kramer MHH, Hoorn EJ, Joles JA, and van Raalte DH**. GLP-1 and the kidney: from physiology to pharmacology and outcomes in diabetes. *Nat Rev Nephrol* 13: 605-628, 2017.
18. **Campos RV, Lee YC, and Drucker DJ**. Divergent tissue-specific and developmental expression of receptors for glucagon and glucagon-like peptide-1 in the mouse. *Endocrinology* 134: 2156-2164, 1994.
19. **Wei Y, and Mojsov S**. Tissue-specific expression of the human receptor for glucagon-like peptide-I: brain, heart and pancreatic forms have the same deduced amino acid sequences. *FEBS Lett* 358: 219-224, 1995.
20. **Bullock BP, Heller RS, and Habener JF**. Tissue distribution of messenger ribonucleic acid encoding the rat glucagon-like peptide-1 receptor. *Endocrinology* 137: 2968-2978, 1996.
21. **Fujita H, Morii T, Fujishima H, Sato T, Shimizu T, Hosoba M, Tsukiyama K, Narita T, Takahashi T, Drucker DJ, Seino Y, and Yamada Y**. The protective roles of GLP-1R signaling in diabetic nephropathy: possible mechanism and therapeutic potential. *Kidney Int* 85: 579-589, 2014.
22. **Hviid AVR, and Sorensen CM**. Glucagon-like peptide-1 receptors in the kidney: impact on renal autoregulation. *Am J Physiol Renal Physiol* 318: F443-F454, 2020.
23. **Pyke C, Heller RS, Kirk RK, Orskov C, Reedtz-Runge S, Kaastrup P, Hvelplund A, Bardram L, Calatayud D, and Knudsen LB**. GLP-1 receptor localization in monkey and human tissue: novel distribution revealed with extensively validated monoclonal antibody. *Endocrinology* 155: 1280-1290, 2014.
24. **Ronn J, Jensen EP, Wewer Albrechtsen NJ, Holst JJ, and Sorensen CM**. Glucagon-like peptide-1 acutely affects renal blood flow and urinary flow rate in spontaneously hypertensive rats despite significantly reduced renal expression of GLP-1 receptors. *Physiol Rep* 5: 2017.
25. **Crajoinas RO, Oricchio FT, Pessoa TD, Pacheco BP, Lessa LM, Malnic G, and Girardi AC**. Mechanisms mediating the diuretic and natriuretic actions of the incretin hormone glucagon-like peptide-1. *Am J Physiol Renal Physiol* 301: F355-363, 2011.
26. **Thomson SC, Kashkouli A, and Singh P**. Glucagon-like peptide-1 receptor stimulation increases GFR and suppresses proximal reabsorption in the rat. *Am J Physiol Renal Physiol* 304: F137-144, 2013.
27. **Rieg T, Gerasimova M, Murray F, Masuda T, Tang T, Rose M, Drucker DJ, and Vallon V**. Natriuretic effect by exendin-4, but not the DPP-4 inhibitor alogliptin, is mediated via the GLP-1 receptor and preserved in obese type 2 diabetic mice. *Am J Physiol Renal Physiol* 303: F963-971, 2012.
28. **Jensen EP, Poulsen SS, Kissow H, Holstein-Rathlou NH, Deacon CF, Jensen BL, Holst JJ, and Sorensen CM**. Activation of GLP-1 receptors on vascular smooth muscle cells reduces the autoregulatory response in afferent arterioles and increases renal blood flow. *Am J Physiol Renal Physiol* 308: F867-877, 2015.
29. **Lee B, Holstein-Rathlou NH, Sosnovtseva O, and Sorensen CM**. Renoprotective effects of GLP-1 receptor agonists and SGLT-2 inhibitors-is hemodynamics the key point? *Am J Physiol Cell Physiol* 325: C243-C256, 2023.
30. **Song P, Huang W, Onishi A, Patel R, Kim YC, van Ginkel C, Fu Y, Freeman B, Koepsell H, Thomson S, Liu R, and Vallon V**. Knockout of Na(+)-glucose cotransporter SGLT1 mitigates diabetes-

induced upregulation of nitric oxide synthase NOS1 in the macula densa and glomerular hyperfiltration. *Am J Physiol Renal Physiol* 317: F207-F217, 2019.

31. **Gorboulev V, Schurmann A, Vallon V, Kipp H, Jaschke A, Klessen D, Friedrich A, Scherneck S, Rieg T, Cunard R, Veyhl-Wichmann M, Srinivasan A, Balen D, Breljak D, Rexhepaj R, Parker HE, Gribble FM, Reimann F, Lang F, Wiese S, Sabolic I, Sendtner M, and Koepsell H**. Na(+)-D-glucose cotransporter SGLT1 is pivotal for intestinal glucose absorption and glucose-dependent incretin secretion. *Diabetes* 61: 187-196, 2012.

32. **Navarro Garrido A, Kim YC, Oe Y, Zhang H, Crespo-Masip M, Goodluck HA, Kanoo S, Sanders PW, Broer S, and Vallon V**. Aristolochic acid-induced nephropathy is attenuated in mice lacking the neutral amino acid transporter B(0)AT1 (Slc6a19). *Am J Physiol Renal Physiol* 323: F455-F467, 2022.

33. **Ge SX, Jung D, and Yao R**. ShinyGO: a graphical gene-set enrichment tool for animals and plants. *Bioinformatics* 36: 2628-2629, 2020.

34. **Babicki S, Arndt D, Marcu A, Liang Y, Grant JR, Maciejewski A, and Wishart DS**. Heatmapper: web-enabled heat mapping for all. *Nucleic Acids Res* 44: W147-153, 2016.

35. **Rieg T, Masuda T, Gerasimova M, Mayoux E, Platt K, Powell DR, Thomson SC, Koepsell H, and Vallon V**. Increase in SGLT1-mediated transport explains renal glucose reabsorption during genetic and pharmacological SGLT2 inhibition in euglycemia. *Am J Physiol Renal Physiol* 306: F188-193, 2014.

36. **Chen L, Chou CL, and Knepper MA**. A Comprehensive Map of mRNAs and Their Isoforms across All 14 Renal Tubule Segments of Mouse. *J Am Soc Nephrol* 32: 897-912, 2021.

37. **Wu H, Kirita Y, Donnelly EL, and Humphreys BD**. Advantages of Single-Nucleus over Single-Cell RNA Sequencing of Adult Kidney: Rare Cell Types and Novel Cell States Revealed in Fibrosis. *J Am Soc Nephrol* 30: 23-32, 2019.

38. **Lake BB, Menon R, Winfree S, Hu Q, Ferreira RM, Kalhor K, Barwinska D, Otto EA, Ferkowicz M, Diep D, Plongthongkum N, Knoten A, Urata S, Mariani LH, Naik AS, Eddy S, Zhang B, Wu Y, Salamon D, Williams JC, Wang X, Balderrama KS, Hoover PJ, Murray E, Marshall JL, Noel T, Vijayan A, Hartman A, Chen F, Waikar SS, Rosas SE, Wilson FP, Palevsky PM, Kiryluk K, Sedor JR, Toto RD, Parikh CR, Kim EH, Satija R, Greka A, Macosko EZ, Kharchenko PV, Gaut JP, Hodgin JB, Consortium K, Eadon MT, Dagher PC, El-Achkar TM, Zhang K, Kretzler M, and Jain S**. An atlas of healthy and injured cell states and niches in the human kidney. *Nature* 619: 585-594, 2023.

39. **Lee JW, Chou CL, and Knepper MA**. Deep Sequencing in Microdissected Renal Tubules Identifies Nephron Segment-Specific Transcriptomes. *J Am Soc Nephrol* 26: 2669-2677, 2015.

40. **Lord CC, Thomas G, and Brown JM**. Mammalian alpha beta hydrolase domain (ABHD) proteins: Lipid metabolizing enzymes at the interface of cell signaling and energy metabolism. *Biochim Biophys Acta* 1831: 792-802, 2013.

41. **Stanton AM, Heydarpour M, Williams JS, Williams GH, and Adler GK**. CACNA1D Gene Polymorphisms Associate With Increased Blood Pressure and Salt Sensitivity of Blood Pressure in White Individuals. *Hypertension* 80: 2665-2673, 2023.

42. **Layton AT, Vallon V, and Edwards A**. A computational model for simulating solute transport and oxygen consumption along the nephrons. *Am J Physiol Renal Physiol* 311: F1378-F1390, 2016.

43. **Barwinska D, El-Achkar TM, Melo Ferreira R, Syed F, Cheng YH, Winfree S, Ferkowicz MJ, Hato T, Collins KS, Dunn KW, Kelly KJ, Sutton TA, Rovin BH, Parikh SV, Phillips CL, Dagher PC, Eadon MT, and Kidney Precision Medicine P**. Molecular characterization of the human kidney interstitium in health and disease. *Sci Adv* 7: 2021.

44. **Kohda Y, Murakami H, Moe OW, and Star RA**. Analysis of segmental renal gene expression by laser capture microdissection. *Kidney Int* 57: 321-331, 2000.

45. **Peterson KS, Huang JF, Zhu J, D'Agati V, Liu X, Miller N, Erlander MG, Jackson MR, and Winchester RJ**. Characterization of heterogeneity in the molecular pathogenesis of lupus nephritis from transcriptional profiles of laser-captured glomeruli. *J Clin Invest* 113: 1722-1733, 2004.

46. **Kang HM, Ahn SH, Choi P, Ko YA, Han SH, Chinga F, Park AS, Tao J, Sharma K, Pullman J, Bottinger EP, Goldberg IJ, and Susztak K**. Defective fatty acid oxidation in renal tubular epithelial cells has a key role in kidney fibrosis development. *Nat Med* 21: 37-46, 2015.
47. **Chen DQ, Chen H, Chen L, Vaziri ND, Wang M, Li XR, and Zhao YY**. The link between phenotype and fatty acid metabolism in advanced chronic kidney disease. *Nephrol Dial Transplant* 32: 1154-1166, 2017.
48. **Rinaldi A, Lazareth H, Poindessous V, Nemazanyy I, Sampaio JL, Malpetti D, Bignon Y, Naesens M, Rabant M, Anglicheau D, Cippa PE, and Pallet N**. Impaired fatty acid metabolism perpetuates lipotoxicity along the transition to chronic kidney injury. *JCI Insight* 7: 2022.
49. **Mohandes S, Doke T, Hu H, Mukhi D, Dhillon P, and Susztak K**. Molecular pathways that drive diabetic kidney disease. *J Clin Invest* 133: 2023.
50. **Wu J, Sun Z, Yang S, Fu J, Fan Y, Wang N, Hu J, Ma L, Peng C, Wang Z, Lee K, He JC, and Li Q**. Kidney single-cell transcriptome profile reveals distinct response of proximal tubule cells to SGLT2i and ARB treatment in diabetic mice. *Mol Ther* 30: 1741-1753, 2022.
51. **Onishi A, Fu Y, Darshi M, Crespo-Masip M, Huang W, Song P, Patel R, Kim YC, Nespoux J, Freeman B, Soleimani M, Thomson S, Sharma K, and Vallon V**. Effect of renal tubule-specific knockdown of the Na(+)/H(+) exchanger NHE3 in Akita diabetic mice. *Am J Physiol Renal Physiol* 317: F419-F434, 2019.
52. **Sun G, da Silva Xavier G, Gorman T, Priest C, Solomou A, Hodson DJ, Foretz M, Viollet B, Herrera PL, Parker H, Reimann F, Gribble FM, Migrenne S, Magnan C, Marley A, and Rutter GA**. LKB1 and AMPKalpha1 are required in pancreatic alpha cells for the normal regulation of glucagon secretion and responses to hypoglycemia. *Mol Metab* 4: 277-286, 2015.
53. **Shackelford DB, and Shaw RJ**. The LKB1-AMPK pathway: metabolism and growth control in tumour suppression. *Nat Rev Cancer* 9: 563-575, 2009.
54. **Pedram A, Razandi M, O'Mahony F, Harvey H, Harvey BJ, and Levin ER**. Estrogen reduces lipid content in the liver exclusively from membrane receptor signaling. *Sci Signal* 6: ra36, 2013.
55. **Chen M, Zhu JY, Mu WJ, Luo HY, Li Y, Li S, Yan LJ, Li RY, and Guo L**. Cdo1-Camkk2-AMPK axis confers the protective effects of exercise against NAFLD in mice. *Nat Commun* 14: 8391, 2023.

Figure legends

Figure 1. Study design and RNA-seq analysis of SGLT2-positive renal proximal tubule cells.

A. Fourteen-week old Sglt1 wildtype (WT) or knockout (KO) mice ± Akita were given vehicle, dapagliflozin or semaglutide for 2 weeks, and SGLT2-positive proximal tubule segments were isolated via immunostaining-guided laser capture microdissection (IS-LCM) followed by RNA sequencing (RNA-seq) analysis. **B.** Laser capture microdissection of SGLT2-positive proximal tubule segments. Frozen kidney sections were stained with anti-SGLT2 antibody and fluorescently labeled SGLT2-positive segments isolated by laser capture microdissection (LCM). Top panels show bright field and bottom panels show fluorescence microscopy of a kidney section before and after IS-LCM. **C.** Confirmation of early proximal tubule enrichment. RNA-seq data of SGLT2-positive segments obtained by IS-LCM in WT mice were compared with reported reference data obtained for all tubular segments (36): relative TPM values in the isolated SGLT2-positive segments for S1 segment marker genes were multi-fold higher than for marker genes of other tubular segments.

Figure 2. Effects of diabetes on the SGLT2-positive proximal tubule transcriptome.

A. Principal component analysis (PCA) of Akita vs WT. **B.** Volcano plot of Akita vs WT. The significance cut-off line is adjusted P value<0.1. **C.** Top 10 affected pathways in Akita vs WT show enrichment of metabolic processes and organic anion transport. **D.** Genes associated with unsaturated fatty acid metabolic process or lipid metabolic process are downregulated in Akita vs WT. **E.** Heatmap of transporter genes (sorted by high to low expression). Expression of 51 transporter genes was deregulated in Akita vs WT, and 48 of them were downregulated while only 3 transporters were upregulated.

Figure 3. Effects of dapagliflozin on SGLT2-positive proximal tubule transcriptome in Akita mice.

A. PCA of Akita+dapagliflozin (dapa) vs Akita. **B.** Volcano plot between Akita+dapa and Akita. **C.** Top 10 enriched pathways with DEGs of Akta+dapa vs Akita. **D.** Correlation plot of two sets of comparisons [(Akita vs WT) and (Akita+dapa vs Akita)]. About 43% genes that are deregulated in Akita were normalized by dapa. **E.** Correlation plot of RNA-seq data and proteomics data. DEGs in Akita+dapa vs Akita positively correlate with protein expression changes. Significantly altered proteins in proteomic analysis (adjusted P<0.1) are denoted (red

dots). **F.** Heatmap of transporter genes that are changed in Akita and restored by dapa. **G.** Heatmap of transporter genes that are not significantly affected in Akita vs WT but altered (all upregulated) by dapa in Akita.

Figure 4. Effects of semaglutide or Sglt1 KO on SGLT2-positive proximal tubule transcriptome in Akita mice.

A. Volcano plot of Akita+semaglutide (sema) vs Akita. **B.** Top 10 enriched pathways by sema treatment in Akita mice. **C.** Ven diagram of two sets of comparisons [(Akita vs WT) and (Akita+sema vs Akita)] shows that ~10% of deregulated genes in Akita were normalized by sema. **D.** Heatmap of transporter genes that are differentially regulated by sema in Akita. Transporters that are deregulated in Akita but normalized by sema are highlighted with red box. Transporters marked with asterisks are regulated in the same way by sema and dapa. **E.** Volcano plot of Sglt1 KO Akita vs Akita. **F.** Heatmap of transporter genes affected by Sglt1 KO in Akita. *Cacna1d* is the only restored gene by loss of SGLT1.

Figure 5. Effects of combined inhibition of SGLT1 and SGLT2 on SGLT2-positive proximal tubule transcriptome in Akita mice.

A. PCA of Sglt1 KO Akita+dapa vs Akita. **B.** Volcano plot of comparison between Sglt1 KO Akita+dapa and Akita. **C.** Ven diagram shows that ~61% of deregulated genes in Akita are normalized by combined Sglt1 KO and SGLT2 inhibition [(Akita vs WT) and (Sglt1 KO Akita+dapa vs Akita)], while SGLT2 inhibition alone restored ~43% [(Akita vs WT) and (Akita+dapa vs Akita)]. **D.** Top 10 pathway enrichments by Sglt1 KO+dapa in Akita. **E.** Heatmap of 28 transporter genes that are restored by Sglt1 KO+dapa in Akita.

Figure 6. Exploring new therapeutic targets in the diabetic early proximal tubule.

A. Heatmap of 61 affected genes in Akita which are unresponsive to dapa, sema, Sglt1 KO or Sglt1 KO+dapa. **B.** Top 5 enriched pathways by 61 unresponsive genes. **C.** Heatmap of 14 transporter genes that are changed by diabetes but not significantly altered in diabetic mice by dapa, sema, Sglt1 KO or Sglt1 KO+dapa. **D.** Correlation between the percentage of restored genes and blood glucose effect by treatment in Akita.

Figure 1.

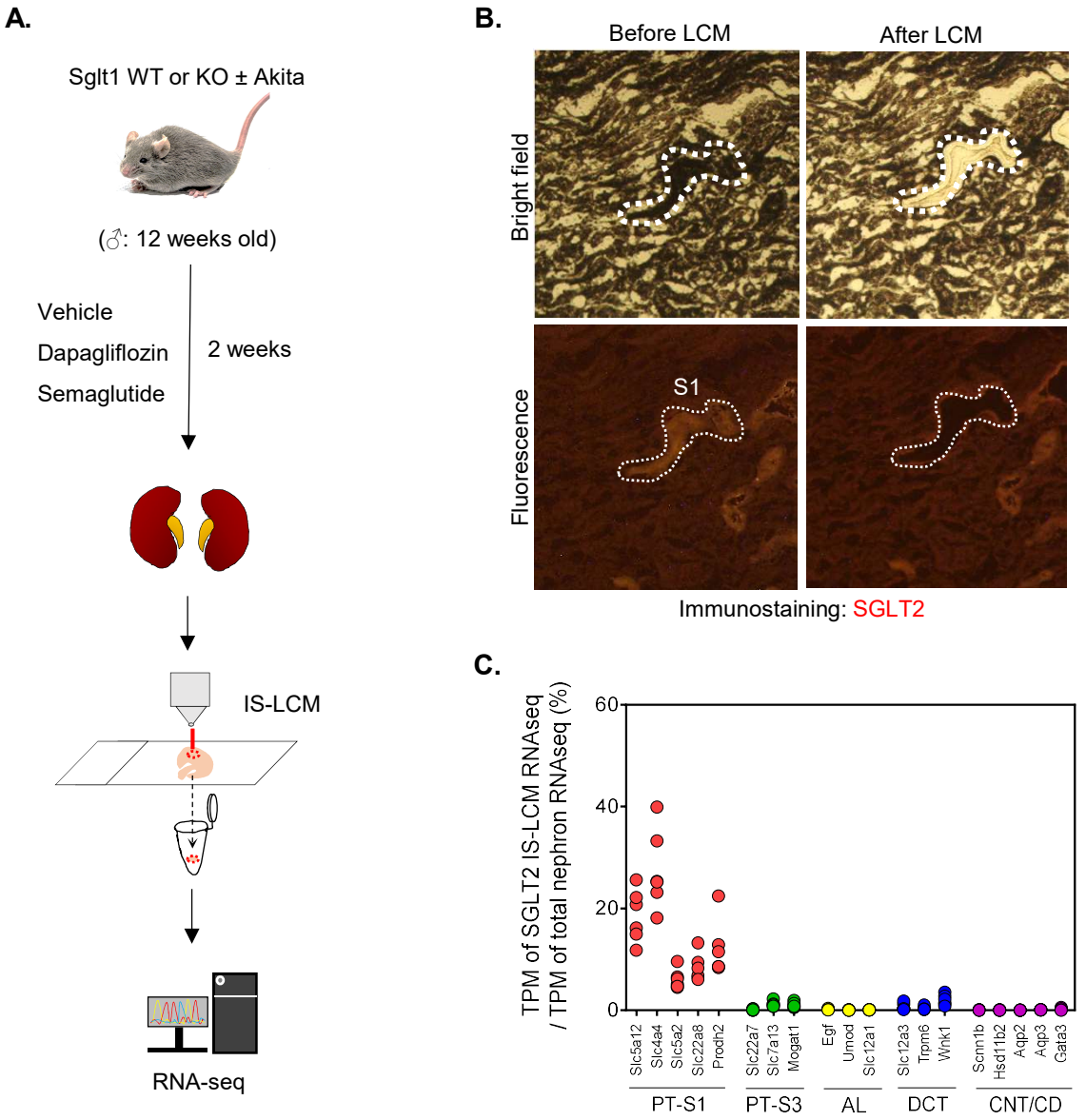
A.
Sglt1 WT or KO ± Akita
(♂: 12 weeks old)
Vehicle
Dapagliflozin
Semaglutide
2 weeks
IS-LCM
RNA-seq
B.
Before LCM
After LCM
Bright field
Fluorescence
S1
Immunostaining: SGLT2
C.
TPM of SGLT2 IS-LCM RNAseq / TPM of total nephron RNAseq (%)
60
40
20
0
Slc5a12
Slc4a4
Slc5a2
Slc22a8
Prodh2
Slc22a7
Slc7a13
Mogat1
Egf
Umod
Slc12a1
Slc12a3
Trpm6
Wnk1
Scnn1b
Hsd11b2
Aqp2
Aqp3
Gata3
PT-S1
PT-S3
AL
DCT
CNT/CD

Figure 2.

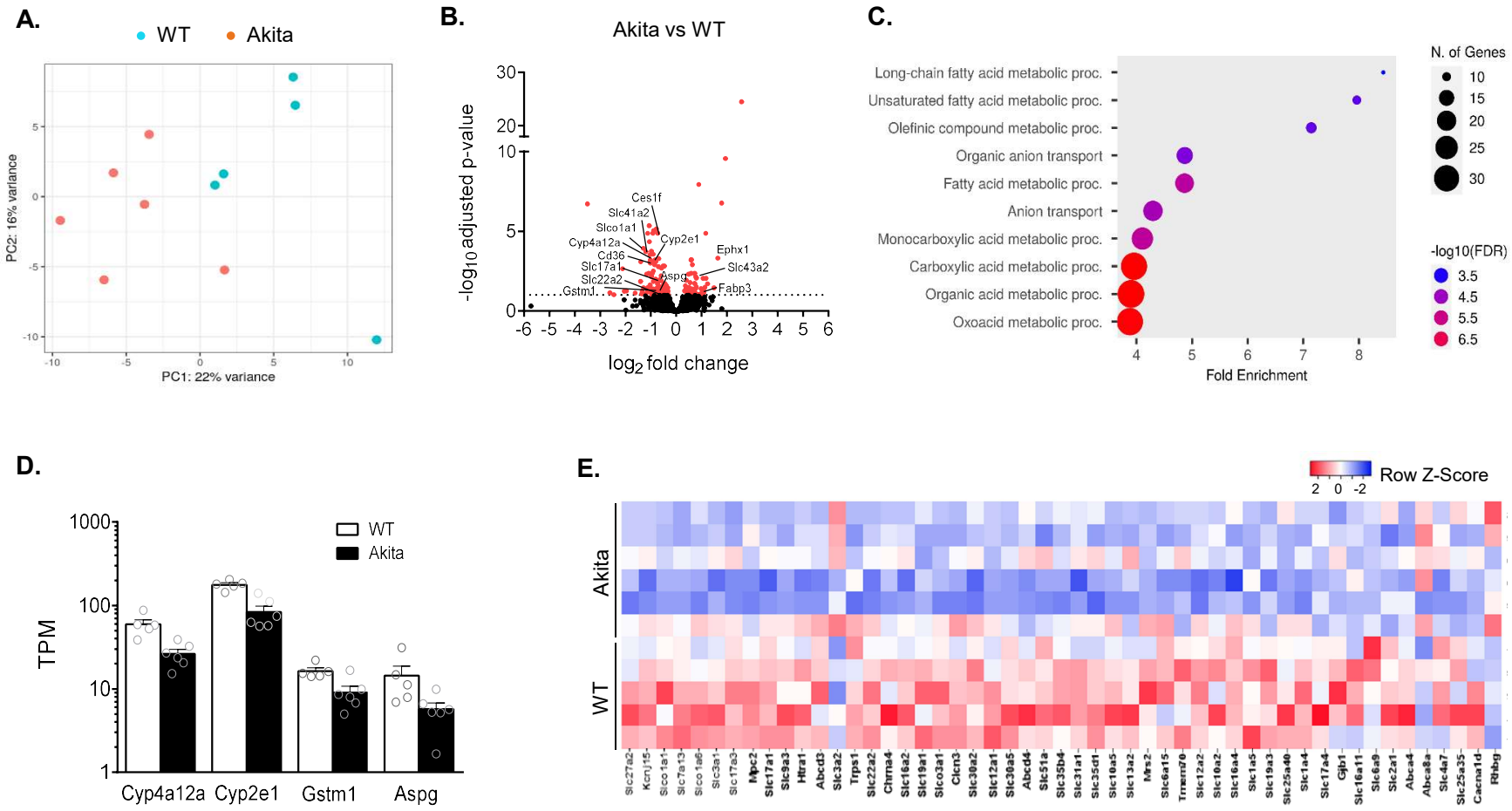
A.
WT
Akita
PC2: 16% variance
PC1: 22% variance
B.
Akita vs WT
-log10 adjusted p-value
log2 fold change
Ces1f
Slc41a2
Slco1a1
Cyp4a12a
Cyp2e1
Cd36
Slc17a1
Slc22a2
Gstm1
Aspg
Ephx1
Slc43a2
Fabp3
C.
Long-chain fatty acid metabolic proc.
Unsaturated fatty acid metabolic proc.
Olefinic compound metabolic proc.
Organic anion transport
Fatty acid metabolic proc.
Anion transport
Monocarboxylic acid metabolic proc.
Carboxylic acid metabolic proc.
Organic acid metabolic proc.
Oxoacid metabolic proc.
Fold Enrichment
N. of Genes
-log10(FDR)
D.
TPM
WT
Akita
Cyp4a12a
Cyp2e1
Gstm1
Aspg
E.
Row Z-Score
Akita
WT

Figure 3.

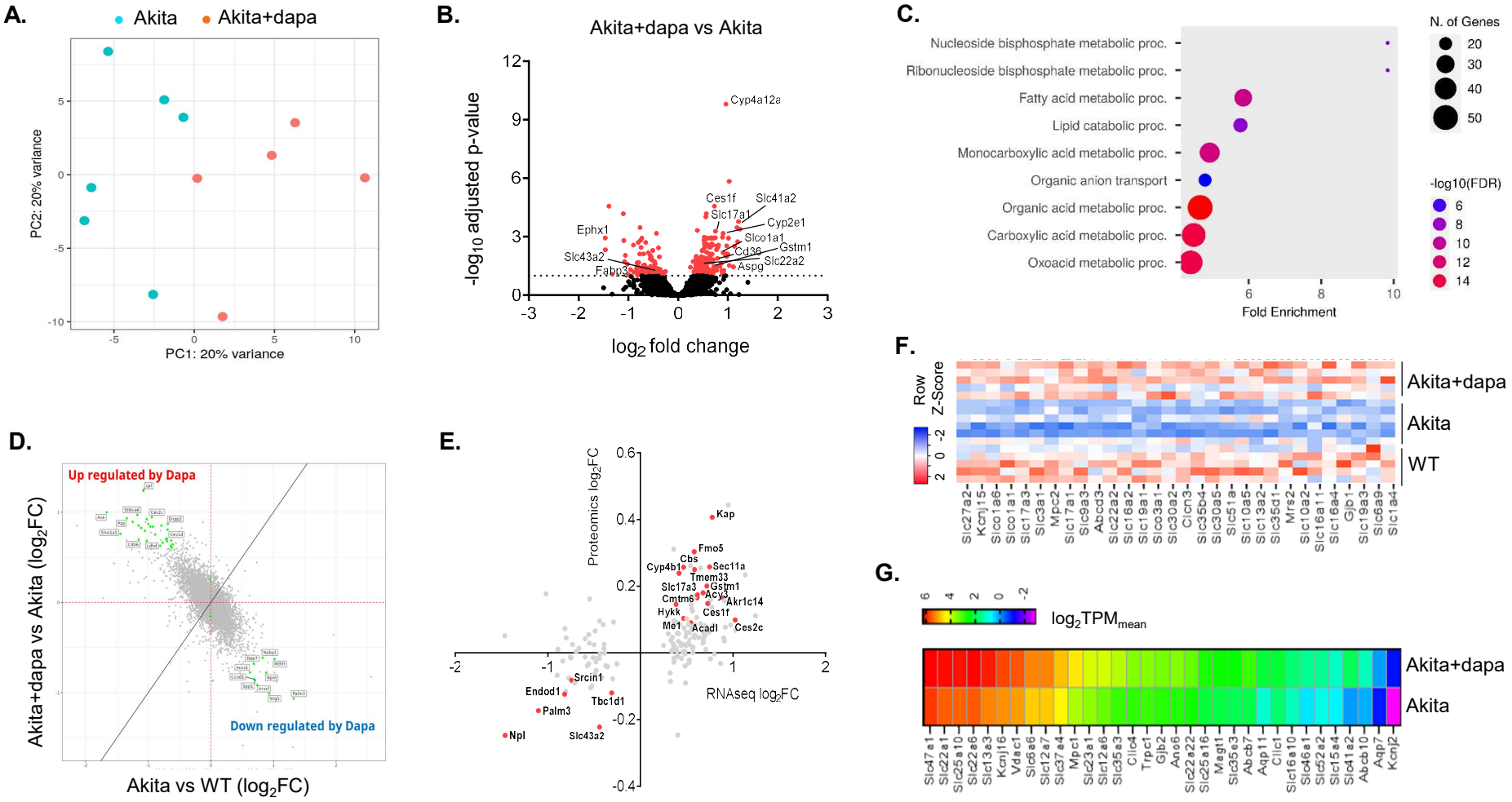
A.
Akita
Akita+dapa
PC2: 20% variance
PC1: 20% variance
B.
Akita+dapa vs Akita
-log10 adjusted p-value
log2 fold change
Cyp4a12a
Ces1f
Slc41a2
Slc17a1
Cyp2e1
Ephx1
Slco1a1
Cd36
Gstm1
Slc43a2
Aspg
Slc22a2
Fabp3
C.
Nucleoside bisphosphate metabolic proc.
Ribonucleoside bisphosphate metabolic proc.
Fatty acid metabolic proc.
Lipid catabolic proc.
Monocarboxylic acid metabolic proc.
Organic anion transport
Organic acid metabolic proc.
Carboxylic acid metabolic proc.
Oxoacid metabolic proc.
Fold Enrichment
N. of Genes
-log10(FDR)
D.
Up regulated by Dapa
Down regulated by Dapa
Akita+dapa vs Akita (log2FC)
Akita vs WT (log2FC)
E.
Proteomics log2FC
RNAseq log2FC
Kap
Fmo5
Cbs
Cyp4b1
Sec11a
Tmem33
Slc17a3
Gstm1
Cmtm6
Akr1c14
Hykk
Ces1f
Me1
Acadl
Ces2c
Srcin1
Endod1
Tbc1d1
Palm3
Npl
Slc43a2
F.
Row Z-Score
Akita+dapa
Akita
WT
G.
log2TPMmean
Akita+dapa
Akita

Figure 4.

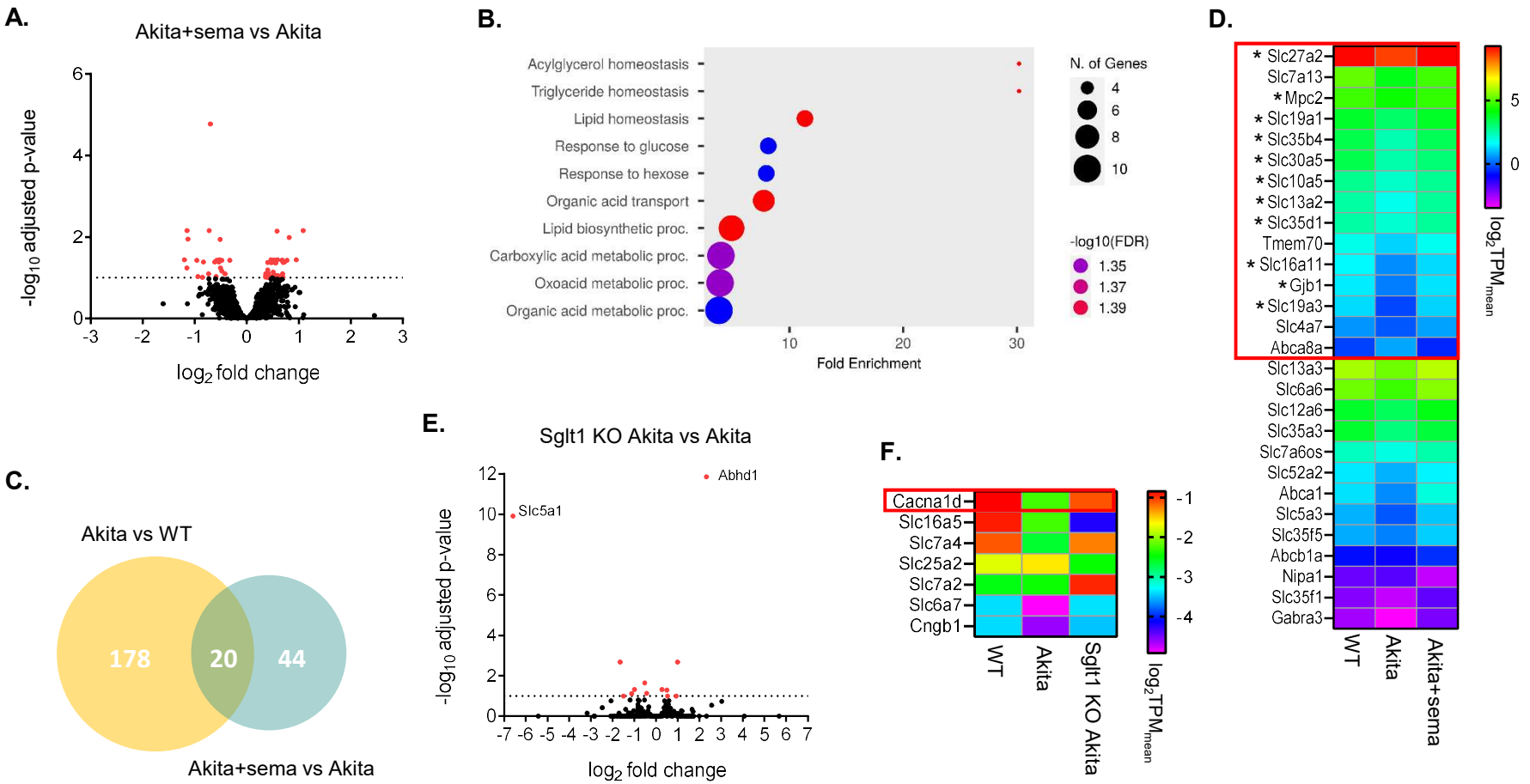
A.
Akita+sema vs Akita
-log10 adjusted p-value
log2 fold change
B.
Acylglycerol homeostasis
Triglyceride homeostasis
Lipid homeostasis
Response to glucose
Response to hexose
Organic acid transport
Lipid biosynthetic proc.
Carboxylic acid metabolic proc.
Oxoacid metabolic proc.
Organic acid metabolic proc.
Fold Enrichment
N. of Genes
-log10(FDR)
C.
Akita vs WT
178
20
44
Akita+sema vs Akita
D.
* Slc27a2
Slc7a13
* Mpc2
* Slc19a1
* Slc35b4
* Slc30a5
* Slc10a5
* Slc13a2
* Slc35d1
Tmem70
* Slc16a11
* Gjb1
* Slc19a3
Slc4a7
Abca8a
Slc13a3
Slc6a6
Slc12a6
Slc35a3
Slc7a6os
Slc52a2
Abca1
Slc5a3
Slc35f5
Abcb1a
Nipa1
Slc35f1
Gabra3
WT
Akita
Akita+sema
log2TPMmean
E.
Sglt1 KO Akita vs Akita
Abhd1
Slc5a1
-log10 adjusted p-value
log2 fold change
F.
Cacna1d
Slc16a5
Slc7a4
Slc25a2
Slc7a2
Slc6a7
Cngb1
WT
Akita
Sglt1 KO Akita
log2TPMmean

Figure 5.

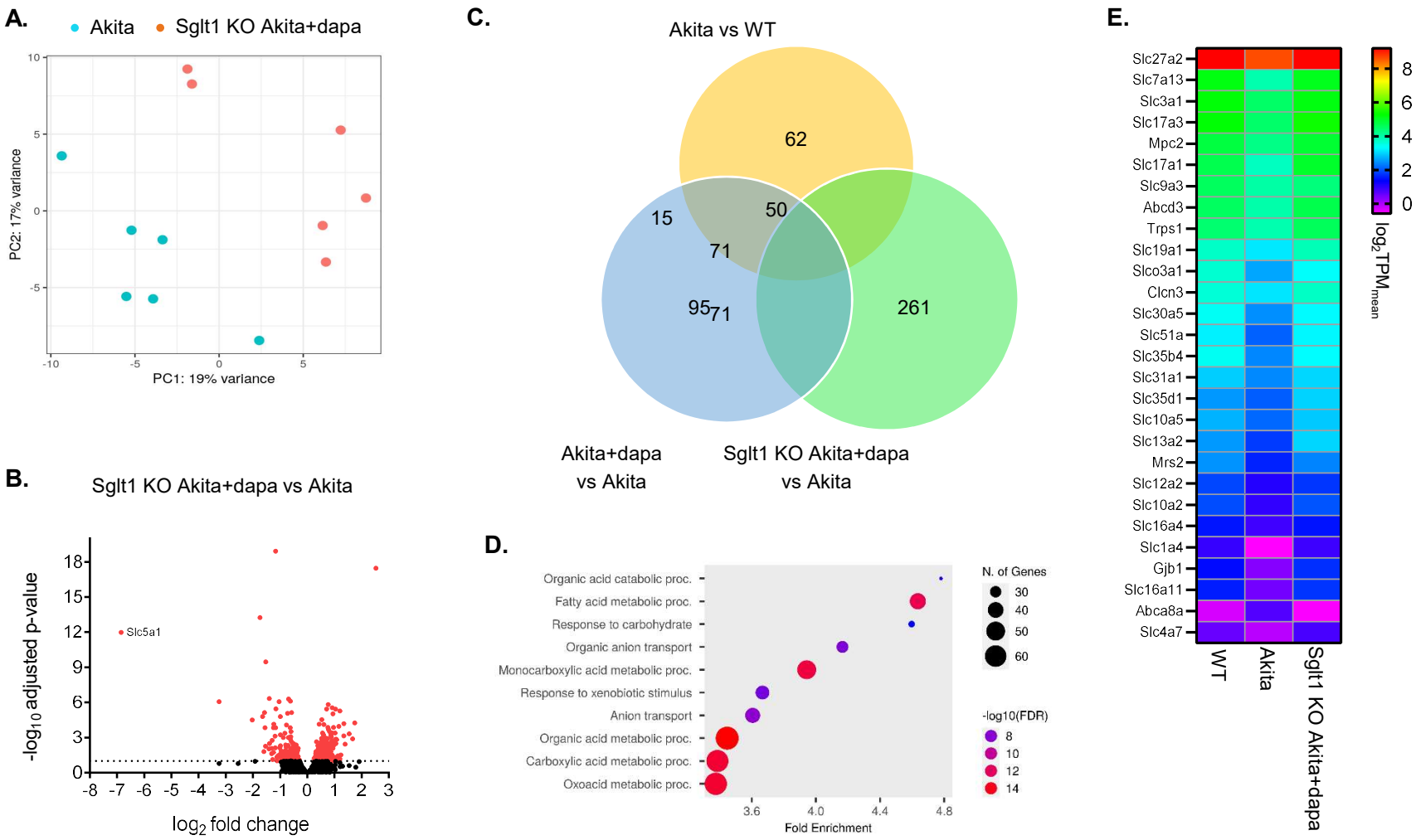
A.
Akita
Sglt1 KO Akita+dapa
PC2: 17% variance
PC1: 19% variance
B.
Sglt1 KO Akita+dapa vs Akita
Slc5a1
-log10 adjusted p-value
log2 fold change
C.
Akita vs WT
62
50
15
71
95
71
261
Akita+dapa
vs Akita
Sglt1 KO Akita+dapa
vs Akita
D.
Organic acid catabolic proc.
Fatty acid metabolic proc.
Response to carbohydrate
Organic anion transport
Monocarboxylic acid metabolic proc.
Response to xenobiotic stimulus
Anion transport
Organic acid metabolic proc.
Carboxylic acid metabolic proc.
Oxoacid metabolic proc.
Fold Enrichment
N. of Genes
-log10(FDR)
E.
Slc27a2
Slc7a13
Slc3a1
Slc17a3
Mpc2
Slc17a1
Slc9a3
Abcd3
Trps1
Slc19a1
Slco3a1
Clcn3
Slc30a5
Slc51a
Slc35b4
Slc31a1
Slc35d1
Slc10a5
Slc13a2
Mrs2
Slc12a2
Slc10a2
Slc16a4
Slc1a4
Gjb1
Slc16a11
Abca8a
Slc4a7
WT
Akita
Sglt1 KO Akita+dapa
log2TPMmean

Figure 6.

A.

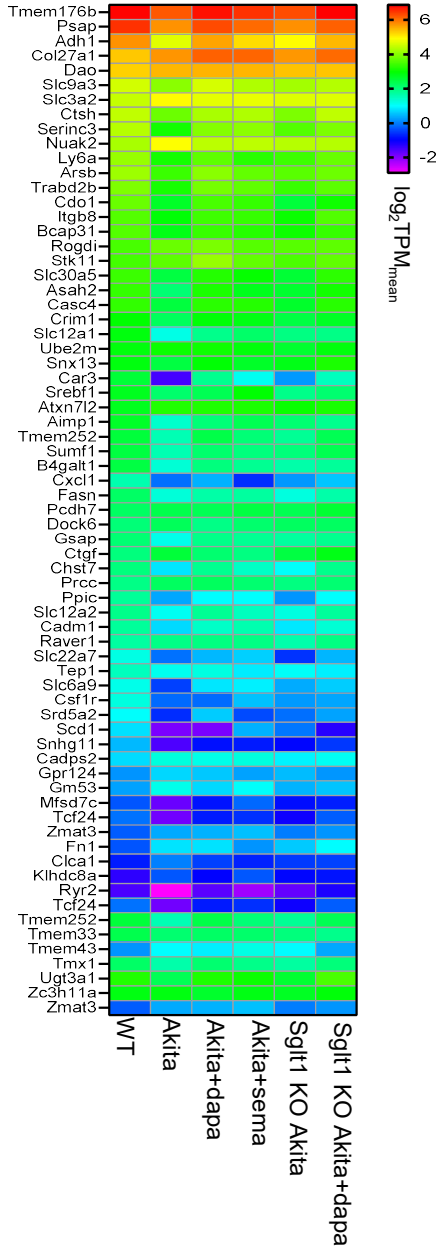

B.

Pathway	FDR	Fold Enrichment	Genes (red, up; black, down)
GO:0033762 response to glucagon	0.03	56.0	Stk11 Srebf1 Cdo1
GO:0006633 fatty acid biosynthetic process	0.093	10.3	Asah2 Fasn Scd1 Srebf1
GO:0006665 sphingolipid metabolic process	0.093	10.7	Asah2 Psap Serinc3 Itgb8
GO:0006814 sodium ion transport	0.093	8.0	Slc6a9 Slc9a3 Slc12a2 Slc12a1 Cxcl1
GO:0006820 anion transport	0.093	5.1	Slc6a9 Psap Slc3a2 Slc12a2 Slc12a1 Clca1 Slc22a7

C.

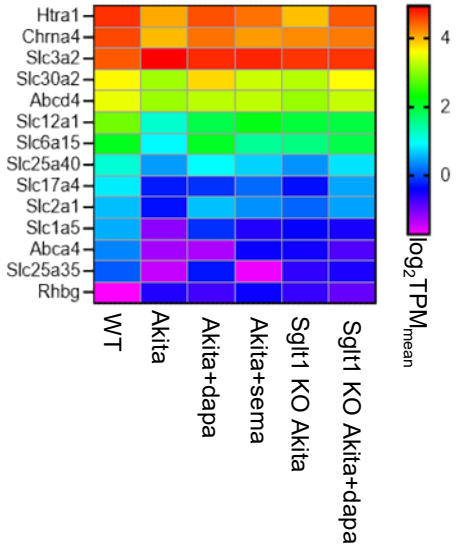

D.

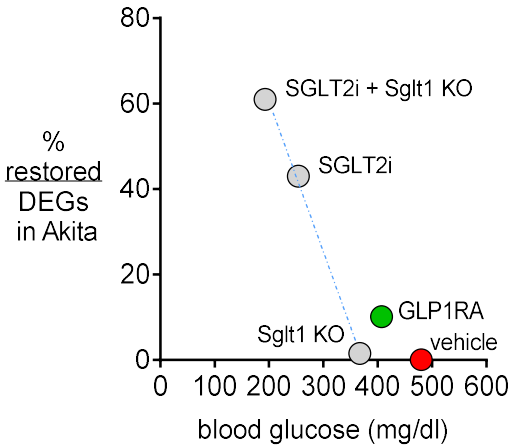

Suppl Figure S1
Part One

Targeted transporter analysis for dapa: transporters whose gene expression in the SGLT2-positive proximal tubule is sensitive to SGLT2 inhibitor dapagliflozin in diabetic mice.

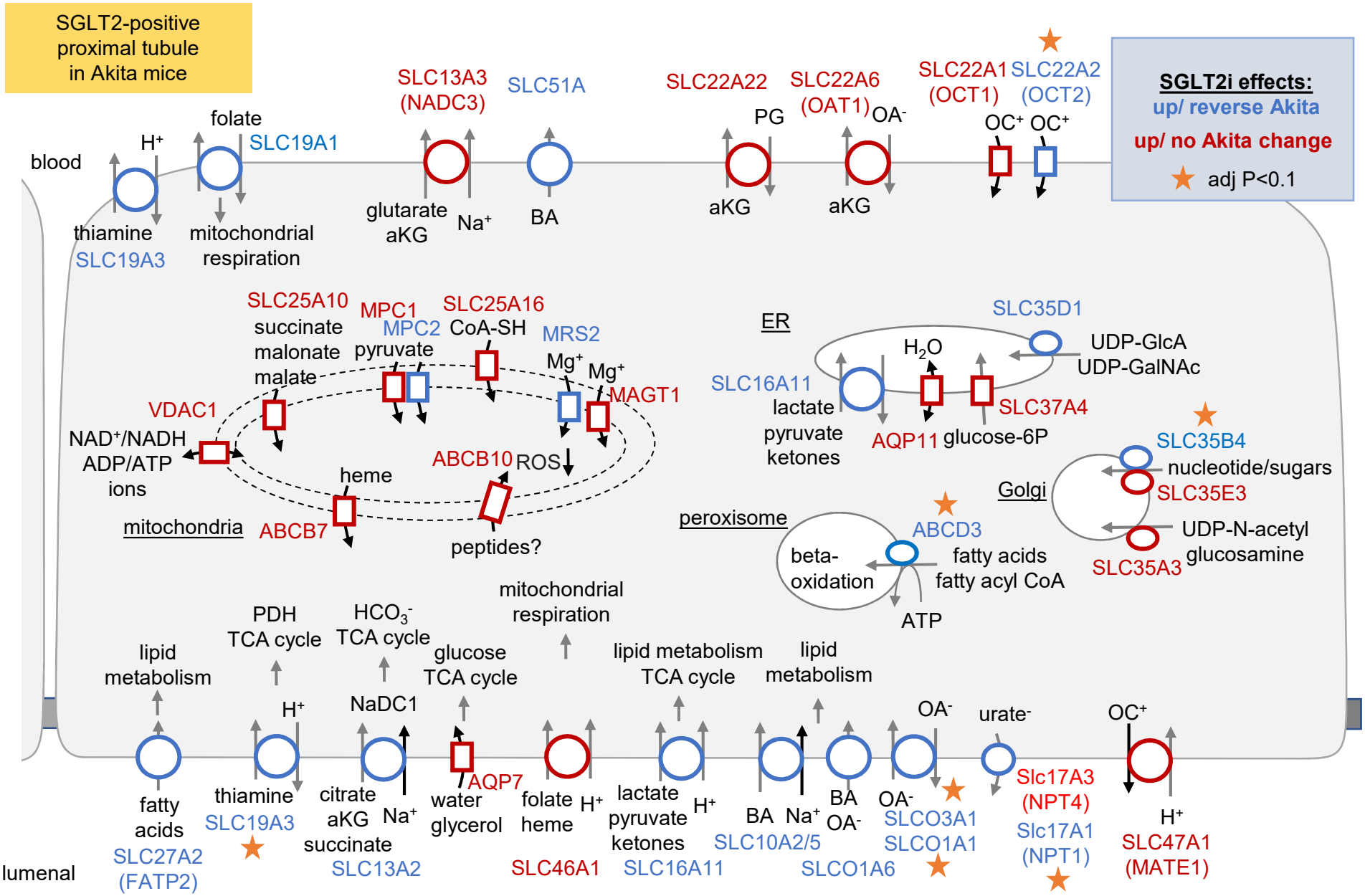

Suppl Figure S1
Part Two

Targeted transporter analysis for dapa: transporters whose gene expression in the SGLT2-positive proximal tubule is sensitive to SGLT2 inhibitor dapagliflozin in diabetic mice.

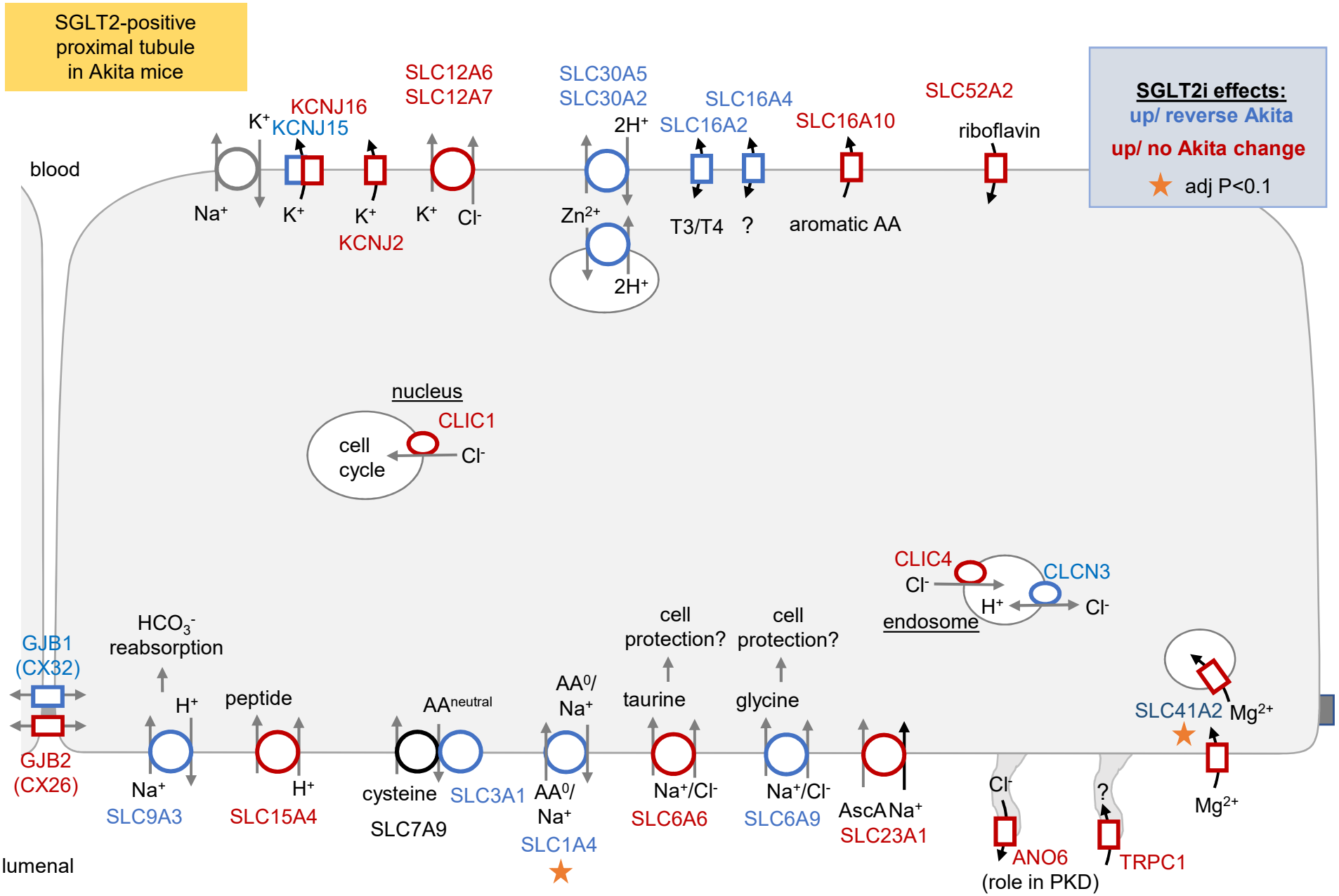

Suppl Figure S2

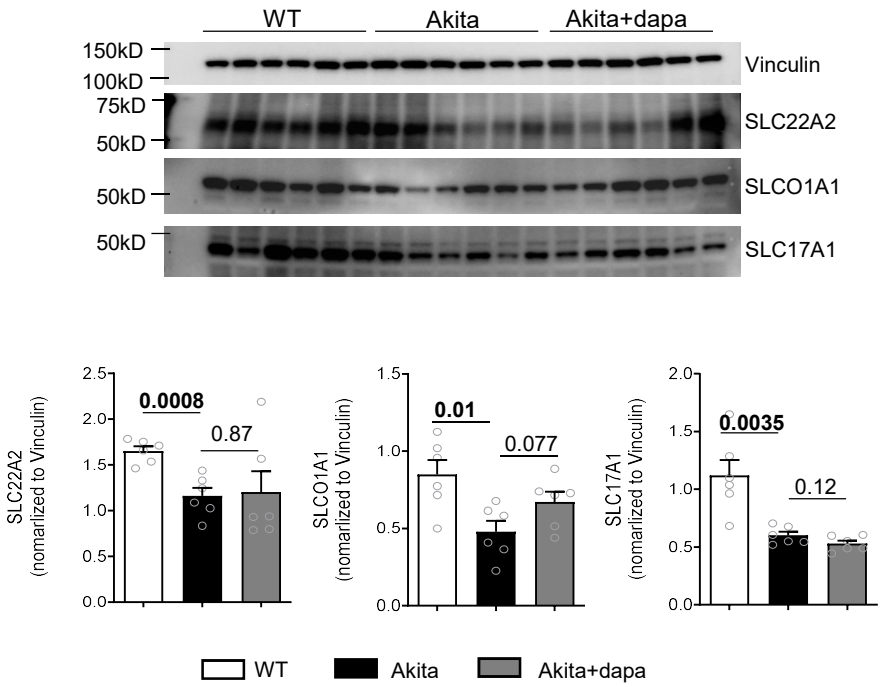

Western blot analysis of transporters in whole kidney membrane fractions. Values are means ± SE, and two-tailed t-test was performed for Akita vs WT or Akita+dapa.

Suppl Figure S3

Genes whose expression in the SGLT2-positive proximal tubule is **restored** by GLP1R agonist semaglutide in diabetic mice.

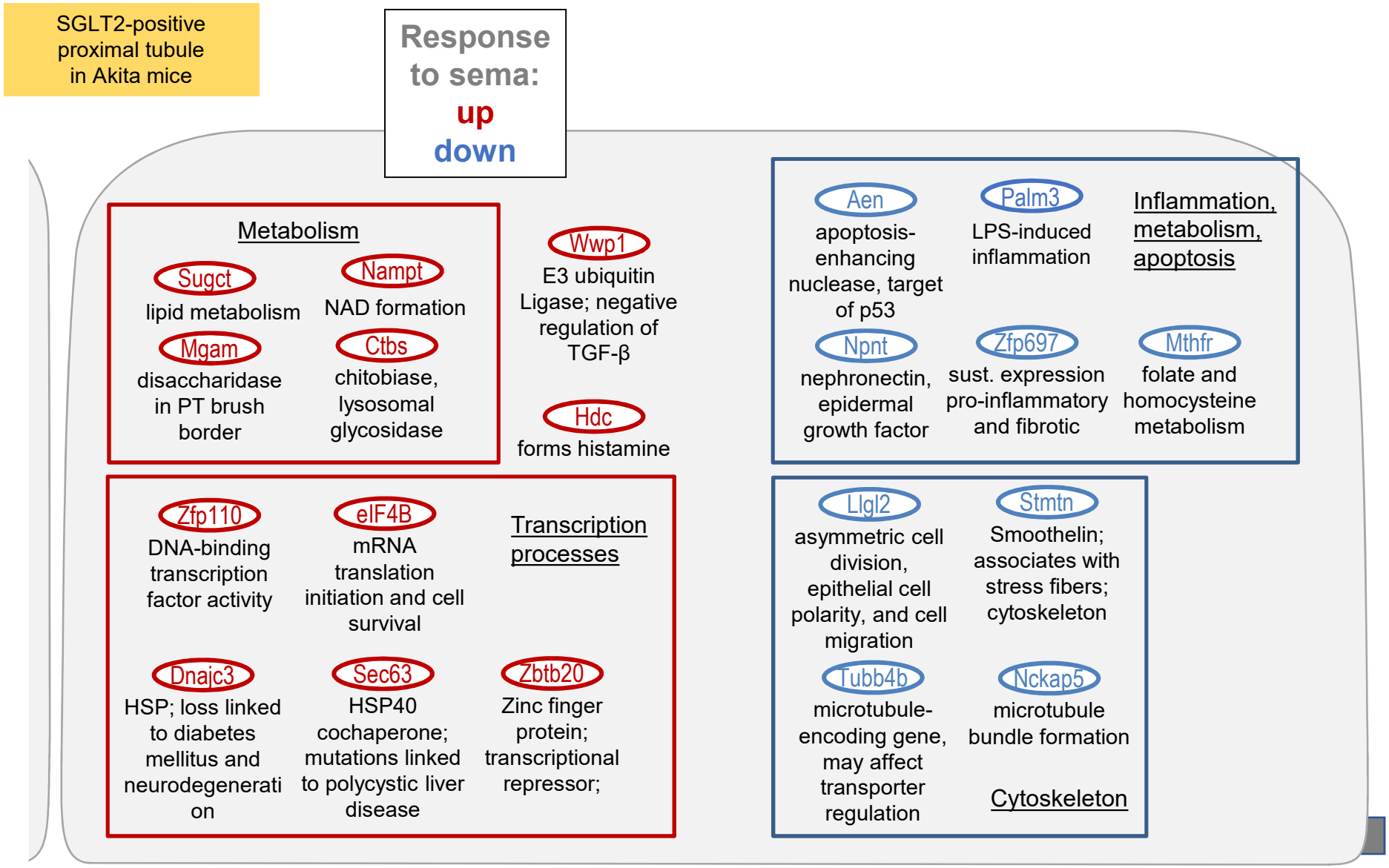

Suppl Figure S4

Targeted transporter analysis for sema: transporters whose gene expression in the SGLT2-positive proximal tubule is sensitive to GLP1R agonist semaglutide in diabetic mice.

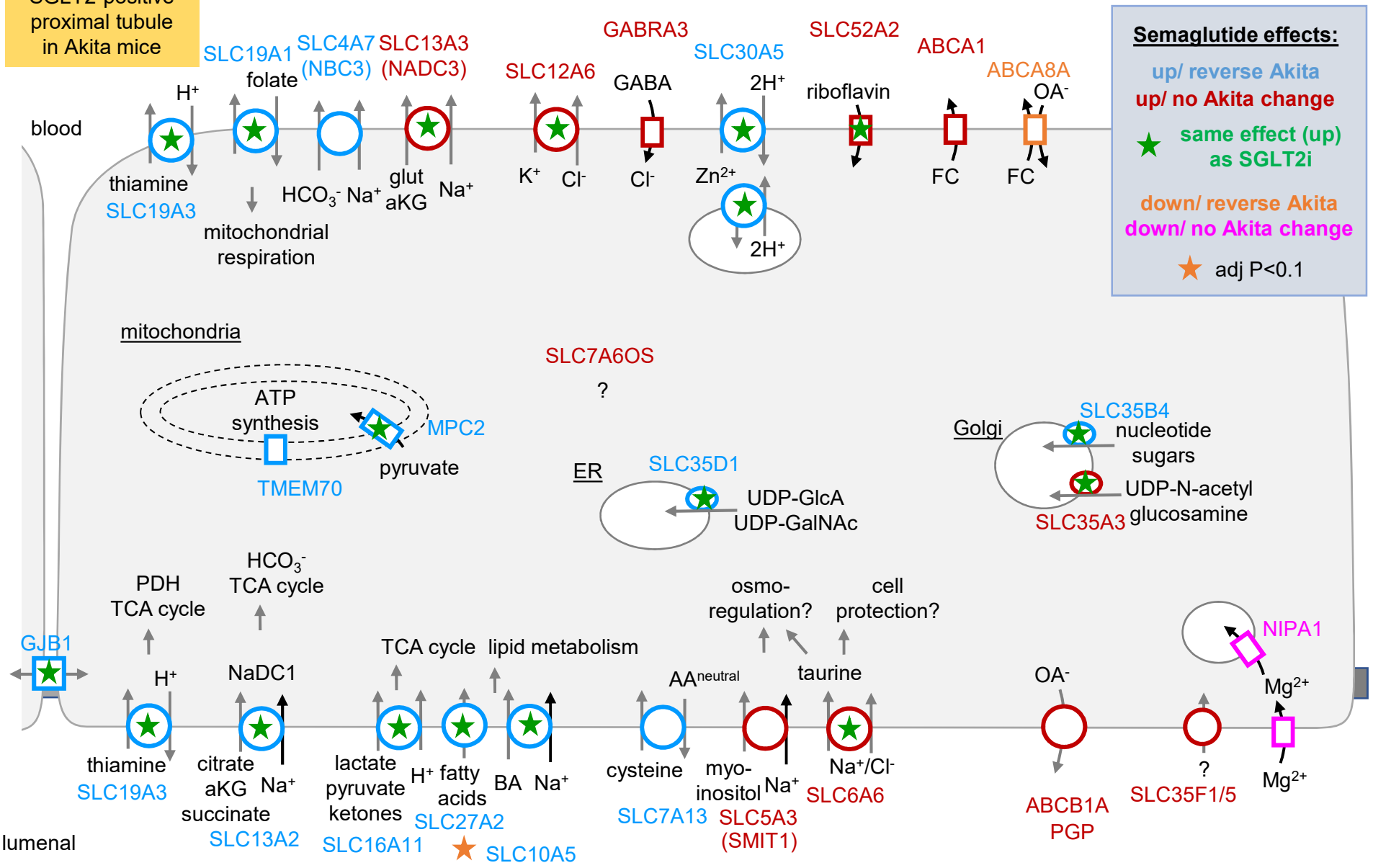

IS-LCM and Transcriptomics of SGLT2-positive early proximal tubules

METHODS

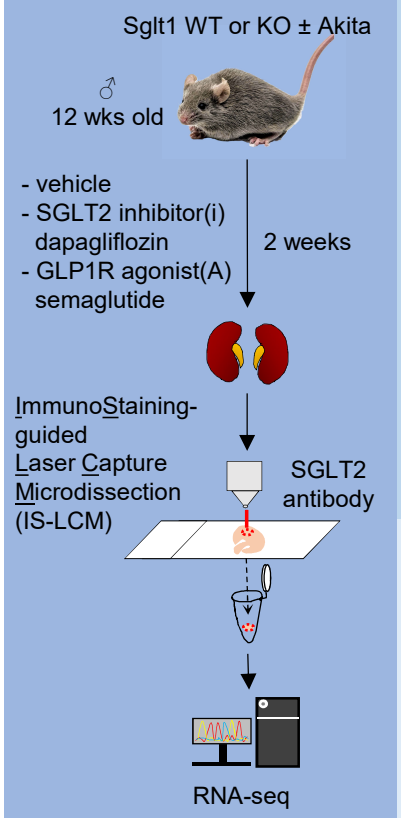

OUTCOME

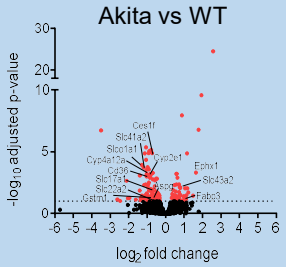

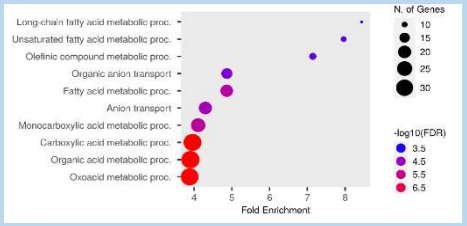

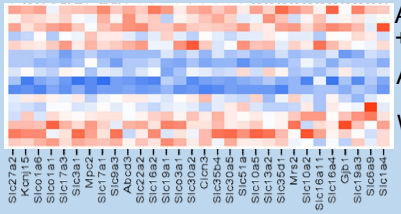

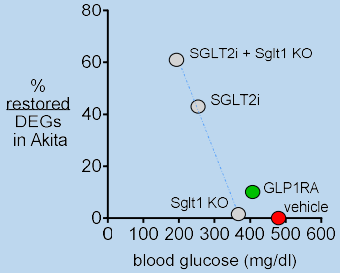

CONCLUSIONS

- Combining IS-LCM of SGLT2-positive segments with RNA-seq identified >20K annotated protein-coding genes.
- ~1% of genes were differentially expressed (DEGs) by Akita including downregulation of fatty acid metabolism and selected transporters.
- SGLT2i restored 43% of DEGs in Akita, and SGLT1&2 inhibition was synergistic possibly due to additive blood glucose effects.
- GLP1RA restored ~10% of DEGs despite small blood glucose effect.